

1 Exploration-based learning of a stabilizing controller 2 predicts locomotor adaptation

3 Nidhi Seethapathi^{1,2}, Barrett Clark³, Manoj Srinivasan^{4,5}

4 ¹Department of Brain and Cognitive Sciences, Massachusetts Institute of Technology, Cambridge, MA 02139

5 ²Department of Electrical Engineering and Computer Science, Massachusetts Institute of Technology, Cambridge,
6 MA 02139

7 ³Bright Machines, Inc., San Francisco, CA 94107

8 ⁴Department of Mechanical and Aerospace Engineering, the Ohio State University, Columbus, OH 43210, USA

9 ⁵Program in Biophysics, the Ohio State University, Columbus, OH 43210, USA

10 ABSTRACT

11 Humans adapt their locomotion seamlessly in response to changes in the body or the environment. We do not understand
12 how such adaptation improves performance measures like energy consumption or symmetry while avoiding falling. Here,
13 we model locomotor adaptation as interactions between a stabilizing controller that reacts quickly to perturbations and a
14 reinforcement learner that gradually improves the controller's performance through local exploration and memory. This model
15 predicts time-varying adaptation in many settings: walking on a split-belt treadmill (i.e. with both feet at different speeds), with
16 asymmetric leg weights, or using exoskeletons — capturing learning and generalization phenomena in ten prior experiments
17 and two model-guided experiments conducted here. The performance measure of energy minimization with a minor cost
18 for asymmetry captures a broad range of phenomena and can act alongside other mechanisms such as reducing sensory
19 prediction error. Such a model-based understanding of adaptation can guide rehabilitation and wearable robot control.

12 Introduction

13 Humans readily adapt their locomotion to diverse environmental conditions and bodily changes^{1–3} (Fig. 1a), but the computational
14 principles underlying such adaptation are not fully understood. While crucial adaptation phenomena have been uncovered
15 through careful experiments^{2,3,3–8} and a handful of models have been proposed to explain individual experiments^{2,9,10}, an
16 integrative understanding of adaptation across paradigms and timescales is missing. Moreover, existing adaptation models are
17 not implemented on a bipedal physics-based agent, and therefore do not encompass the stability-critical nature of adapting
18 locomotion while avoiding falling. In this work, we put forth an integrative model of locomotor adaptation combining stabilizing
19 control, performance-improving reinforcement learning, and performance-based memory updates. Our model predicts
20 locomotor adaptation phenomena across paradigms in ten prior studies and two prospective experiments conducted in this study.

21 Theories of motor adaptation have predominantly been developed for discrete episodic tasks such as reaching with the
22 arm^{11–13}. Adaptation principles that explain such episodic tasks may not be sufficient for explaining continuously cascading
23 stability-critical tasks such as locomotion, multi-fingered manipulation, and many activities of daily living. In episodic tasks like
24 reaching where the arm's state is re-set at the end of each episode, the errors during one episode do not dynamically propagate
25 to the next episode. In contrast, in continuously cascading tasks like locomotion, errors can have short-term and long-term
26 consequences to stability unless otherwise controlled^{14–17}. Prior accounts of locomotor adaptation^{2,9,18} do not consider the
27 interaction with locomotor dynamics, perhaps assuming that dynamic stability is ensured by a distinct mechanism. For instance,
28 metabolic energy reduction-based accounts^{2,19} treated adaptation to be a univariate optimization process – implicitly assuming
29 that changes on one step do not affect the next step through the dynamics. Similarly, error-based learning models developed
30 for arm reaching^{11–13}, when applied to locomotor adaptation^{9,10,18,20,21}, do not usually interact with the locomotor dynamics;
31 these models fit the kinematic symmetry error transients, without considering how these errors might affect stability. Here, we
32 put forth a model that explains how humans adapt continuously during walking while maintaining dynamic stability.

33 Improving some aspect of performance is a driving force for motor adaptation and learning. However, we do not
34 understand which performance objectives explain diverse locomotor adaptation phenomena. Minimization of different types of
35 error^{11,12,22–24} (e.g., sensory prediction error, task error, proprioceptive conflict) or minimization of metabolic energy^{2,7,8,25}
36 have been separately posited as performance objectives underlying locomotor adaptation. However, these performance
37 objectives often do not generalize across settings. Metabolic energy minimization can explain steady state adaptation in some
38 experimental settings^{25,26} but does not in other settings²⁷. Similarly, while error-based learning models can be fit to asymmetry

39 changes in some tasks^{3,4,6,10,18,24}, they cannot make predictions for tasks where there is no changes in the symmetry^{28,29}. A
40 computational model that precisely specifies the performance objectives such as energy, sensory prediction error, proprioceptive
41 conflict, etc. would help identify the performance objectives that predict locomotor adaptation phenomena across tasks. Here,
42 we put forth such a predictive model of locomotor adaptation allowing comparisons between the predictive ability of difference
43 performance objectives, finding that energy minimization predicts the broadest range of phenomena.

44 In this work, we contribute a model of adaptation which causally links the body dynamics, stabilizing control policy,
45 learning algorithm, performance goal, internal model of performance, and memory of control. We model adaptation as an
46 exploration-driven gradient-based improvement of a stabilizing controller, explaining how humans improve their locomotor
47 performance continuously while maintaining stability. Our model predicts adaptation phenomena in ten prior experimental
48 studies and two model-guided experiments conducted here. The model captures learning phenomena such as fast timescale
49 response followed by slow timescale adaptation, savings, faster de-adaptation, generalization, non-learning in some situations,
50 and the effect of noise and prior experience. By modifying the performance objective, we show that our modeling framework
51 can help compare theories of locomotor adaptation such as minimizing energy, sensory prediction error (via proprioceptive
52 realignment), or kinematic task error (e.g., asymmetry) in their ability to explain phenomena.

53

54 Results

55 A modular and hierarchical model of locomotor adaptation

56 We posit a modular and hierarchical model of locomotor adaptation (Fig. 1b-d) in which a controller keeps the human stable,
57 a gradient-based reinforcement learner modifies this stabilizing controller to improve performance, an internal model learns
58 to predict performance in a new environment, and a memory mechanism stores the improved walking strategies and deploys
59 them when advantageous. The model is modular in that there are separate but interacting modules performing distinct tasks
60 (stabilizing control, gradient estimation, gradient-based learning, memory update); the model is hierarchical in that some
61 modules operate at and explain phenomena at distinct timescales that are hierarchically separated. We test the ability of the
62 computational model to predict experimentally observed locomotor adaptation phenomena in a number of experiments: see our
63 repository *LocAd*³⁰ for the code implementing the model.

64 A critical constraint on human locomotion is being stable i.e. not falling down, despite internal and external perturbations.
65 Thus, a stabilizing controller forms the inner-most level of our hierarchical model^{16,17,31} (Fig. 1b). We posit that during
66 locomotion in a familiar setting, humans use a previously learned controller, which we call a ‘default controller,’ stored as a
67 motor memory. We further posit that the structure of this default controller constrains how humans adapt to a novel situation.
68 We characterized this default controller by modeling how humans respond to small deviations from nominal walking on the
69 treadmill^{16,17,31}. This controller can be decomposed into a feedforward component, not dependent on the biped’s state, and
70 other state-dependent feedback terms (see *Methods*). We used effectively the same initial default controller for all the locomotor
71 adaptation tasks considered here (see *Methods* and *Supplementary Methods*). This is possible because the controller is robust to
72 substantial noise and uncertainty as we have previously shown^{16,17}, allowing the human to move stably in novel environments.

73 It has been hypothesized that the nervous system chooses movements that optimize some performance objective, for
74 instance, reducing energy expenditure^{8,32-36} or reducing left-right asymmetry^{3,18,24,37} (Fig. 1b). We posit that when faced
75 with a novel circumstance, humans gradually change their default stabilizing controller to optimize performance. This
76 performance improvement is achieved through gradient-based reinforcement learning in an outer loop around the stabilizing
77 controller (Fig. 1b,c). We found that allowing the reinforcement learner to adapt just the feedforward terms of the controller,
78 leaving the stabilizing feedback terms unchanged, is sufficient to explain the observed phenomena. The learner estimates the
79 gradient descent direction using ‘intentional’ exploratory noise^{2,13,38} in the neighborhood of the default controller, contributing
80 to increasing the step-to-step variability^{16,17,31}. While the term ‘reinforcement learning’ has a multitude of algorithmic
81 specifications³⁹, here we use this term as shorthand for the proposed local exploration-based learning algorithm.

82 Motor adaptation involves memorization and retrieval of control policies. Here, we posit a module in the outer loop that
83 forms longer-term motor memories^{40,41} of the controllers being learned, parameterized by the settings in which they were
84 learned. This stored memory is used when encountering a setting similar to one previously encountered (Fig. 1b,d), interpolating
85 and generalizing between settings via function approximation³⁹. Stored memory is only used when it may improve performance
86 and does not conflict with gradient descent (Fig. 1d). Conversely, stored memory is updated when the current controller’s
87 performance is better than that of the motor memory. See *Methods* and the model’s implementation in code, *LocAd*³⁰, for
88 further details.

89 We have posited that the gradual modification of a stabilizing controller for performance optimization is a primary mecha-
90 nism for locomotor adaptation. Adaptation may also result from other mechanisms such as recalibration to reduce sensory
91 prediction error^{11,22,42,43}. Here, we extend the aforementioned framework, showing that the model can incorporate sensory
92 error-based adaptation mechanisms, replacing the feedback controller of Fig. 1b by a more general sensorimotor transformation

93 (see Fig. 9 and *Methods*).

94

95 **Predicting fast and slow timescale learning in many locomotor settings**

96 The model predicted locomotor adaptation phenomena in many different conditions, including a split-belt treadmill, an
97 asymmetrically added leg mass, external assistance, exoskeleton-based perturbations, and abrupt treadmill speed changes (Fig.
98 2). For the reinforcement learner, we tested minimizing four performance objectives: only energy expenditure, only asymmetry
99 (specifically, step length asymmetry, defined below), a weighted sum of energy and asymmetry, and a kinematic task error.
100 For the results below, we use energy expenditure alone or energy expenditure with a small step length asymmetry penalty as
101 the performance objective as these give qualitatively similar results, we use the latter when the performance objective is not
102 explicitly mentioned. Minimization of other objectives are discussed in their own separate sections later.

103 The most popular experimental paradigm used to investigate human locomotor adaptation is walking on a split-belt
104 treadmill^{4,6,7,44}, which has two side-by-side belts that can be run at different speeds. Most humans have never experienced this
105 novel situation. Humans adapt to walking on a split-belt treadmill on the timescale of seconds, minutes, and hours, exhibiting
106 stereotypical changes in their walking motion^{1,45,46} and the model predicts these changes (Fig. 2a).

107 Specifically, within a few strides of split-belt walking, humans start walking with high negative step length asymmetry^{4,44} –
108 that is, the step length onto the slow belt is longer than the step length onto the fast belt (see Fig. 2a and Supplementary Fig. 1e).
109 This is the fastest timescale of adaptation, sometimes called ‘early adaptation.’ This negative step length asymmetry becomes
110 close to zero over a few hundred strides (about ten minutes), and then becomes slightly positive with more time⁷. The model
111 predictions have all these fast and slow transients both when minimizing just energy or energy plus a step length asymmetry
112 (Fig. 2a and Fig. 8a). The model predicts an immediate initial increase in energy cost upon encountering the split-belt condition,
113 which then reduces to a lower steady state gradually, as found in prior experiments⁶. When the split-belt condition is removed,
114 the model predicts a fast-timescale transient to large positive step length asymmetry (a learning after-effect) and then a slow
115 de-adaptation back to normal walking. The model predicts this de-adaptation to be faster than the adaptation, as found in
116 experiments^{4,7,44} (Fig. 2a). The model also predicts that steady state is reached more quickly for step time asymmetry, and
117 that the energy cost is more sensitive to step time asymmetry compared to step length asymmetry (Supplementary Fig. 3), as
118 suggested by some prior experiments^{6,47}.

119 Human adaptation proceeds analogously when they are made to walk with an extra mass attached asymmetrically to just
120 one ankle, as characterized by a prior experiment⁵. The model predicts the qualitative features of such adaptation, whether the
121 performance objective is just energy or has an additional symmetry term (Fig. 2b). In both experiments⁵ and in our model, the
122 walking gait becomes asymmetric in step lengths and then, during slow timescale adaptation, gradually tends toward symmetry;
123 when the extra mass is removed, the asymmetry jumps to the opposite side, and then gradually de-adapts to normal walking.

124 The model predicts the step frequency changes while walking at varying speeds on a ‘tied-belt’ treadmill – which is just
125 regular treadmill with one belt, or equivalently, a split-belt treadmill with equal belt speeds (Fig. 2c). In prior experiments²⁸ in
126 which the belt speed was changed every 90 seconds, humans quickly adapt their step frequency within 2 seconds and then
127 slightly adjust their step frequency over a longer timescale — with the initial fast transient either overshooting or undershooting
128 the ultimate steady state frequency slightly. In previous work²⁸, the overshooting and undershooting transients required separate
129 fits, whereas our model predicts both with the same framework.

130 The model captures empirical findings of how humans adapt to exoskeleton assistance. In some prior experiments^{29,48},
131 humans were provided with time-periodic ankle torque impulses via a robotic exoskeleton (Fig. 2d). If the time period of
132 these external impulses was close to the human stride period and the impulse magnitude was in the right range, the humans
133 changed their stride frequency to entrain to this external impulse frequency, as predicted by the model (Fig. 2d-ii). Both
134 model and experiment show entrainment that approximately aligns the external impulse with the transition from one step to
135 the next (Fig. 2d-iii). The model can show entrainment whether the external impulse frequency is faster or slower than the
136 stride frequency^{29,48}, as found in prior experiment, while some prior models have shown that entrainment²⁹ is possible for
137 higher frequencies with just a feedback controller without learning. Rather than provide such time-periodic assistance, if the
138 external assistive forces from the exoskeleton are a simple function of current body state (and not too noisy), the learner predicts
139 successful adaptation toward the new optimum (Supplementary Fig. 4). We consider other such exoskeleton adaptation studies
140 later in this manuscript (e.g., Fig. 4).

141

142 **Lesions in simulation identify modules responsible for the fast and slow adaptation transients**

143 We can analyze which hypothesized modules in the model are responsible for explaining specific observations by the computa-
144 tional analog of ‘lesion experiments’: that is, turning off specific modules and noting what experimentally observed adaptation
145 feature is degraded or lost. The following observations apply to all but the exoskeletal entrainment of the previous section, but
146 we center the discussion on split-belt walking.

147 The fastest transient (early adaptation i.e., the initial response immediately upon experiencing the new condition) is entirely

148 due to the default controller and the natural dynamics of the biped. Turning off both the reinforcement learner and the memory
149 mechanism still results in the fast timescale initial response due to the stabilizing controller (Fig. 4a). Recent experiments
150 partially corroborate this prediction, showing that providing gait stability through other means (e.g., handrail) affects this initial
151 transient^{49,50}, though such experiments may have changed other aspects of the gait than just stability.

152 Turning off the default stabilizing controller by setting all feedback gains to zero often makes the biped fall to the ground
153 when the novel condition is initiated. Lowering the feedback gains to near zero results in falling or substantially degraded
154 learning (Fig. 3a-b). Thus, the stabilizing controller is critical for effective locomotor adaptation. Further, this exercise of
155 lowering the feedback gains closer to zero leaves a large fraction of the initial transients intact – showing that the feedforward
156 component of this default controller is substantially responsible for the initial transient (Fig. 3a).

157 The slow adaptation transient when first exposed to the novel condition is due to the reinforcement learner improving
158 performance. Turning off the reinforcement learner and the memory mechanism with zero learning rates results in the fast
159 timescale initial response due to the stabilizing controller (Fig. 4a), but no slow timescale adaptation response. Thus, the
160 stabilizing controller alone cannot explain the slow transients. Turning on the reinforcement learner results in the slow timescale
161 adaptation response. Changing the learning rate for the reinforcement learner modulates the speed of this slow adaptation (Fig.
162 4b). In the first exposure to these novel situations, there is not yet any memory to call upon, and therefore, memory specific to
163 the novel situation does not contribute to the first adaptation.

164 De-adapting to a familiar situation (equal belt speeds) after exposure to a novel situation will involve the use of stored
165 memory of the familiar situation. Specifically, in split-belt walking, our model predicts that the de-adaptation will be faster than
166 adaptation due to the use of stored motor memory of walking with tied-belts (Fig. 2a)^{6,45}. Turning off this memory use, the
167 de-adaptation is slower than adaptation (Fig. 4c). During first adaptation to a novel setting, the slow transients are governed by
168 gradient descent, whereas during de-adaptation back to a familiar setting, the slow transients are sped up due to the summing of
169 gradient descent and progress toward stored memory (Fig. 1d).

170

171 **Explaining savings, generalization, and anterograde non-interference**

172 ‘Savings’ refers to the faster re-learning of a task that has previously been experienced. In prior experimental work, such
173 faster re-learning during a second split-belt adaptation experience was observed^{1,51}, despite having a prolonged tied-belt
174 period between the two adaptation periods (Fig. 5) — this intervening tied-belt period allows for full ‘washout’, complete
175 de-adaptation in terms of observable variables. Here, our model qualitatively predicts such empirically observed savings (see
176 Fig. 5 and Supplementary Table 1 for statistics). Such faster re-learning in the model is due to the motor memory mechanism,
177 which stores how the controller changes under different situations. Motor memories are formed during first exposure to a novel
178 condition, and then when exposed to this condition again, the re-learning is faster due to gradient descent and memory use
179 acting synergistically (Fig. 1d). Because the motor memories are task-dependent, memories for split-belt adaptation do not
180 decay entirely during tied-belt washout as the two tasks are non-overlapping. This persistent memory from the first exposure to
181 split-belt walking results in the observed savings.

182 ‘Generalization’ is when adaptation under one task condition results in savings or faster adaptation for a different task
183 condition. Humans exhibit generalization during locomotor adaptation and our model predicts this phenomenon (Supplementary
184 Fig. 6a-b). Specifically, in one prior experiment⁵², humans exposed to a split-belt trial A showed savings for a split-belt trial
185 B with a smaller speed difference between both belts than A. Thus, experience with task A sped up adaptation to task B,
186 suggesting that humans generalized from A to B. Further, it was observed⁵² that such savings for task B from experiencing task
187 A (with the larger belt-speed difference) was higher than the savings obtained if the first adaptation experience was with task B
188 instead. Our model predicts both these generalization phenomena (Supplementary Fig. 6a-b) due to the motor memory being
189 continuously parameterized with respect to continuous-valued task parameters (here, belt speeds), so that the controller for
190 intermediate conditions are interpolated even if they are never directly encountered. Such generalization cannot be predicted by
191 models in which memories are stored discretely without interpolation².

192 ‘Anterograde interference’ is when adapting to one task makes you worse at adapting to the ‘opposite’ task: opposite
193 locomotor adaptation tasks could be split-belt walking tasks with belt speeds switched. Contrary to arm reaching adaptation
194 studies where such anterograde interference is observed⁴¹, our model predicts that such interference need not happen in
195 locomotion: that is, adapting to one perturbation need not make you worse at adapting to the ‘opposite’ perturbation if there is a
196 sufficient tied-belt washout period between the two adaptation phases (Fig. 6a). This non-interference can be explained by the
197 memory mechanism incorporating a function approximation, so that it can meaningfully extrapolate the learned controllers to
198 the opposite perturbation as well. Such non-interference was indeed found in prior locomotor experiments⁵¹.

199 To further test the model’s predictions on how prior experience shapes adaptation, we performed prospective experiments
200 here: we tested adaptation to two opposite split-belt tasks A and B without a washout period (see Fig. 6b), while prior
201 experiments had a substantial washout period between the split-belt phases⁵¹. We found that the model predicted both the
202 increased initial step length asymmetry transient due to the recent adaptation to the opposite task and the insignificant changes

203 to adaptation time-constants (see Fig. 6b and Supplementary Table 1 for comparisons and statistics).

204 More generally, our model qualitatively captures effects of different split-belt adaptation protocols, for instance, capturing
205 the time course of step length asymmetry when the split-belt phase is introduced gradually or abruptly, and whether these
206 adaptation phases are short or extended^{18,20} (Supplementary Fig. 5). Having a longer duration adaptation phase in which the
207 perturbation grows gradually may sometimes result in less savings than a shorter adaptation phase in which the perturbation
208 began abruptly and remains constant (Supplementary Fig. 5). In previous work, an explicit memory of errors was used to
209 explain some of these results⁹, but we have provided an alternative explanation via different model assumptions. In these cases
210 (Supplementary Fig. 5), we found that the adaptation to different kinds of exposure to gradual and abrupt conditions can depend
211 on protocol-specific parameters (e.g., duration of different phases, perturbation magnitude, learning rates); this suggests that
212 one must be cautious of claiming general trends based on limited experiments.

213 The model predicts how the size and duration of perturbations affects adaptation^{1,18,52}. In split-belt walking, both in model
214 and in prior experiment⁵², being exposed to a larger belt-speed split results in larger initial transients and more positive final
215 asymmetry (Supplementary Fig. 6c). Being exposed to a condition for a shorter period of time results in smaller savings than
216 being exposed to the condition for longer¹⁸ (Supplementary Fig. 5).

217 **Degraded learning, non-learning, and making non-learners adapt via experience**

218 The human motor system has sensory noise and motor noise that is not fully observable, and is thus distinct from intentional
219 exploratory noise. The results presented thus far were obtained with low levels of sensorimotor noise. When the sensorimotor
220 noise is less than a critical threshold, it preserves the qualitative results despite degrading the gradient approximation and
221 thus degrading the effective learning rate (Fig. 4d). Large enough sensorimotor noise for fixed exploratory noise destroys
222 the reinforcement learning entirely, resulting in no kinematic adaptation or energy reduction upon first exposure (Fig. 4d),
223 potentially explaining why some populations with movement disorders may have impaired learning⁵³.

224 Prior adaptation experiments involving exoskeleton assistance found that some humans were able to adapt spontaneously
225 whereas others did not^{2,8,27}. The non-spontaneous learners, when exposed to broad experience with a lower associated
226 metabolic cost, were able to adapt toward the energy optimum^{2,8}. In our model, both spontaneous learning and non-learning
227 was possible depending on the size of sensorimotor noise: low noise resulted in spontaneous learning and high noise resulted in
228 non-learning. As in experiment^{2,8}, the model's non-learners could be made to adapt toward a lower energy cost by giving them
229 broad experience on the energy landscape, giving them experience of a lower energy cost to be stored in memory. In our model,
230 this adaptation upon providing experience stems from motor memory formation and later memory use in addition to improving
231 performance through gradient descent.

232 In addition to intrinsic sensorimotor noise, adaptation to external devices such as exoskeletons or treadmills could also
233 be degraded by 'device noise'. Our model predicts that split-belt adaptation can be degraded via such device noise when
234 implemented as noisy belt speed fluctuations that are large enough (Fig. 7a). To test this model prediction prospectively,
235 we performed human subject experiments and compared the post-adaptation after-effects of noise-free and noisy split-belt
236 protocols. We found that participants had lower after-effects after the noisy adaptation condition, as predicted by the model; see
237 Fig. 7a and Supplementary Table 1. This device-noise-based degradation may seem in conflict with earlier experiments by
238 Torres-Oviedo and Bastian²⁰, who compared adaptation in a split-belt protocol under noise-free and noisy belt speed conditions
239 and found that the noisy version had higher adaptation as judged by the post-adaptation after-effects. However, our model
240 also captures this improved adaptation due to different implementation of device noise in prior experiments²⁰ by incorporating
241 that specific protocol in the model (Fig. 7b), thus reconciling the seemingly conflicting findings. These results illustrate that
242 the details of the noise pattern (e.g., magnitude and temporal correlations, see *Methods*) and the adaptation protocol used are
243 important to determine the impact of device noise on adaptation, i.e., there are many ways to add device noise and some may
244 enhance learning and others may degrade it.

245 Aside from noise-based explanations, we provide one more potential cause for initial non-learning observed in some
246 exoskeleton studies: delay between human action and exoskeleton response. Many exoskeleton adaptation experiments in
247 which participants did not spontaneously adapt^{2,8,27} had an exoskeleton controller that provided assistance or resistance based
248 on the participant's previous walking step, resulting in a delay between action and energetic consequence. We showed that such
249 delays can degrade or even stop gradient descent-based learning (Supplementary Fig. 7), making adaptation not obligatory.
250 The gradient estimate is degraded due to poor credit assignment: when there is delay, the reinforcement learner in our model
251 associates the effect with an incorrect cause, as the learner's inductive bias assumes no such delays.

252 **Alternative to energy minimization: Comparing to minimizing asymmetry**

253 To explain split-belt adaptation, researchers have treated the left-right asymmetry in step length as the error being corrected,
254 fitting equations with one or two time constants to describe the observed decrease in this asymmetry^{1,9,10}. Here, we examined
255 what predictions our model makes if step length asymmetry is used in our optimization framework as the only performance

258 objective, a variant of another study²⁴ in which foot contact time symmetry was optimized. We find that minimizing asymmetry
259 does not capture the slow timescale transients in either tied-belt or split-belt locomotion. First, for changing treadmill speeds
260 during tied-belt locomotion²⁸, minimizing asymmetry predicts the fast timescale changes in step frequency due to the default
261 controller, but further slow timescale changes observed in experiment are not predicted by an asymmetry-minimizing objective
262 alone. During split-belt adaptation, minimizing just step length asymmetry, our model predicts convergence to pure step length
263 symmetry (Fig. 8a). This is in contrast to recent experiments which suggest eventual convergence to positive step length
264 asymmetry⁴⁵. In general, minimizing asymmetry is insufficient as the lone performance objective in an optimization framework,
265 as perfect symmetry admits infinitely many locomotion patterns⁵⁴ and does not result in isolated local minima required for
266 stereotypy. Thus, minimizing asymmetry alone cannot predict the many steady state locomotor phenomena predicted by
267 minimizing energy during normal locomotion^{28,33,55}. As a corollary, when placed in any symmetric situation with a symmetric
268 body (e.g., slopes or bilaterally symmetric exoskeletons), minimizing asymmetry will result in zero slow timescale adaptation
269 of the controller even if the mechanical environment is changed substantially, in contrast to experimental findings^{2,8,27}. While
270 minimizing asymmetry alone does not explain diverse locomotor phenomena, minimizing a heuristically weighted combination
271 of energy and asymmetry, with a small weight on the asymmetry, retains the qualitative predictions of minimizing energy, while
272 sometimes allowing a better quantitative match (Fig. 2a-b and Fig. 8a). Future experiments could delineate the extent to which
273 humans have symmetry as an explicit objective in addition to energy⁵⁶, given that energy⁵⁴ and other performance objectives
274 such as proprioceptive realignment (as shown below) may also indirectly promote symmetry^{22,42}.

275

276 Alternative to energy minimization: Comparing to minimizing generalized task error

277 In low-dimensional adaptation tasks such as reaching with the arm to a target, the task error to be minimized is unambiguous;
278 for instance, in reaching tasks with visuomotor rotation, the error is defined as angular distance to the reach target^{9,12}. However,
279 in higher-dimensional tasks like locomotion, analogous definitions of task error as deviation from desired body kinematics
280 is not uniquely defined: for instance, the total task error could be defined as a weighted sum of the error from desired body
281 states, with errors for different states weighted differently — but such a weighting would not be uniquely specified. Here, we
282 considered a few such relative weightings and made model predictions for minimizing such kinematic task errors as the only
283 performance objective (see *Methods* and Fig. 8b) via the exploration-driven gradient descent of Fig. 1b.

284 The resulting predictions were not entirely consistent with experiment. Different relative weightings resulted in distinct
285 behaviors, all of which fell short of fully capturing the experimental findings: the weighting that results in eventual positive step
286 length asymmetry, as seen in experiment, corresponded to energy increase in contrast to experiments, and on the other hand, the
287 weighting that results in monotonic energy decrease has a steady state with substantial negative step length asymmetry, again in
288 contrast to experiments (Fig. 8c). A purely kinematic performance objective was similarly found to not explain exoskeleton
289 adaptation in prior experiments, where participants achieved entrainment to exoskeleton impulses⁴⁸ or changed their walking
290 frequency⁸ without plateauing at the unassisted walking kinematics.

291

292 Alternative to performance optimization: Comparison with proprioceptive realignment

293 Proprioceptive realignment has been proposed as a potential mechanism accounting for the adaptation seen in split-belt
294 locomotion^{22,42} and for arm reaching tasks with visuomotor perturbations^{57,58}. Vasquez et al⁴² characterized the (proprio-
295 perceptively) perceived speed of the legs after a split-belt adaptation, effectively finding that humans perceived the fast leg as
296 being systematically slower than reality or the slow leg as faster than reality or both. A causal mechanism relating this sensory
297 recalibration to locomotor adaptation has not previously been proposed, and a mathematical model could help establish if
298 proprioceptive realignment could result in symmetry changes consistent with experiment.

299 We put forth a mathematical model of proprioceptive realignment via sensory recalibration using our framework, which
300 enables linking body dynamics, sensory feedback (both proprioception and vision), and motor action. In our model, the two
301 legs are expected to be on the same surface and proprioceptive deviations from this sensory prediction are perceived as an
302 error to be corrected by recalibrating proprioception; while only proprioception is recalibrated, vision is used as a common
303 sensory signal to estimate the proprioceptive conflict between the two legs (see *Methods* and Fig. 9a). This is a type of sensory
304 prediction error^{12,58}, as it is due to a difference between the sensory feedback and what the nervous system expects. This model
305 results in recalibrated estimates of leg speeds such that on a split-belt treadmill, the fast leg feels slower and slow leg feels
306 faster than reality, as in experiment⁴² (Fig. 9c), with the recalibration growing in time. The model produces no recalibration
307 when walking on a tied-belt, as in experiment⁴². We incorporated this recalibrating proprioceptive sensing as feedback input to
308 the stabilizing controller without changing other aspects of the default controller to predict what proprioceptive realignment
309 alone can predict.

310 Proprioceptive realignment as implemented here falls short of explaining qualitative features of split-belt locomotor
311 adaptation. Specifically, while the initial negative step length asymmetry produced by the default controller is decreased
312 by proprioceptive realignment, the steady state of the adaptation still has substantial negative asymmetry (Fig. 9d), falling

313 substantially short of experimentally observed symmetry^{6,59} and positive step length asymmetry^{7,45}, which is predicted by
314 energy optimization. Interestingly, the model shows coincidental metabolic energy decrease as a result of proprioceptive
315 realignment (Fig. 9e), but this energy decrease is not accompanied by kinematic changes observed in experiment. Thus, while
316 proprioceptive realignment could potentially be a partial cause of split-belt adaptation, it does not explain all the associated
317 adaptation phenomena, as also suggested by recent experiments⁶⁰. Beyond split-belt adaptation, proprioceptive realignment
318 cannot explain how humans respond to tied-belt speed changes²⁸, as experiments did not find significant proprioceptive
319 realignment in the tied-belt condition⁴². Finally, proprioceptive realignment via interaction with vision, as implemented here,
320 cannot explain adaptation to purely mechanical changes to the body or the environment such as an added mass or an exoskeleton.

321

322 **Interaction with explicit feedback**

323 Our framework is meant to model implicit adaptation and learning, but can accommodate explicit adaptation mechanisms
324 acting in parallel. One potential way to speed up locomotor adaptation is to provide explicit verbal instruction to the participant
325 about the desired behavior or provide visual feedback on the error between desired and actual behavior¹⁰ (Fig. 10a). Indeed,
326 providing visual feedback on step length asymmetry to participants on a split-belt treadmill and asking them to reduce this
327 asymmetry hastened the progress toward symmetry — compared to adaptation without this feedback¹⁰. Removing this visual
328 feedback partway through adaptation results in the increased symmetry being largely wiped out, so that the asymmetry goes
329 back approximately to where it would have been without the explicit feedback. We were able to capture this phenomenon (Fig.
330 10c-d) by adding a separate module for explicit control that acts in parallel to the feedback controller in memory (Fig. 10a), as
331 hypothesized in some prior work^{10,23}. This demonstration is simply to show that the implicit learner of Fig. 1b can be readily
332 modified to accommodate explicit mechanisms without degrading the implicit learner’s performance. This demonstration also
333 shows that kinematic behavior changes due to explicit corrections need not, by themselves, be sufficient to modify implicit
334 learning, as seen in experiments^{10,21}.

335

336

337 **Discussion**

338 We have presented a model for locomotor adaptation that captures observed experimental phenomena in ten different studies^{3–8,18,20,28,48,51,52}, and predicts phenomena observed in two prospective experiments conducted in this study. Across
339 these studies, our model captures adaptation transients in both the short timescale of seconds and long timescale of many
340 tens of minutes. Our model also enabled us to compare different adaptation mechanisms, specifically energy optimization
341 via reinforcement learning, proprioceptive realignment, and reducing sensory prediction error^{22,42,58,61}, delineating how the
342 hypotheses differ or coincide in their predictions and allowing testing through future prospective experiments. We have shown
343 how humans could adapt to perturbations to the body or the environment, while walking stably and continuously without falling
344 or stopping, as models of non-continuous episodic tasks such as arm reaching do not show how this is possible.

345 Predictive models of motor learning such as the one proposed here could be used to improve motor learning in the real
346 world. We have made predictions about conditions that may degrade or accelerate learning consistent with prior experiments.
347 Given this, future hypotheses for improving learning could be tested computationally within our modeling framework before
348 testing via prospective experiments. We have tested the model by performing two such prospective experiments here, one for
349 examining anterograde interference and another for the effect belt noise. Further such experiments may either provide further
350 evidence supporting the model or information that could help improve the model. If the goal is to improve learning to use a
351 device (such an exoskeleton or a treadmill), the device parameters and their sequencing can be optimized in simulation to
352 reduce the time duration to learning steady state.

353 Our model suggests explanations for why humans may adapt reliably in some novel situations (for instance, during split-belt
354 walking^{4,6,20}) and not others (for instance, some exoskeleton studies^{2,8,19,62}). One might wonder if common principles underlie
355 such reliable adaptation in one class of devices and unreliable adaptation in another class, given that both devices are interacting
356 with the same human motor control system. First, we note that both exoskeletons and split-belt treadmills share a core dynamical
357 similarity: they are both mechanical devices that contact the body, applying forces and performing positive or negative work of
358 different specifications⁴⁵. Second, our results also suggest that the two classes of devices are not fundamentally different with
359 respect to motor learning, but that the differences may be due to dynamical properties of treadmills versus current exoskeletons
360 and their controllers. Our model suggests ways in which we can make participants less reliable learners on split-belt treadmills
361 and reliable learners on exoskeletons and prostheses. Specifically, our model predicts that split-belt adaptation can be degraded
362 by noisy belt speed variations (Fig. 7) — which we confirmed with our prospective experiment. We also noted that many
363 exoskeleton studies that did not show obligatory adaptation involved exoskeleton controllers that had a one step delay between
364 human action and the device response^{2,8,19}. We showed that gradient descent can be substantially degraded or entirely stopped
365 in the presence of such delays (Supplementary Fig. 7), whereas there can be reliable learning in exoskeletons with no delay

367 or noise (Supplementary Fig. 4); this prediction can be tested by systematically manipulating the device delay in future
368 experiments. In summary, we suggest that humans may exhibit better adaptation to exoskeletons if the device has low noise, has
369 simple consistent dynamics from step to step, and does not have substantial delay between human action and device response.

370 A corollary to the prediction that lowering device noise improves learning reliability is that increasing baseline human
371 exploratory variability compared to unresolved sensorimotor or device noise may improve learning reliability. It is an open
372 question whether baseline exploration as used by the nervous system in implicit learning can be manipulated by an experimenter
373 via purely external means (that is, via sensory or mechanical perturbations or other biofeedback) — in a manner that results
374 in more reliable learning. One study that increased variability externally did not find better learning⁶³, while another study performed a
375 increased learning²⁰: our model was able to recapitulate the increased learning in the latter study. Another study performed a
376 manipulation that increased both variability and learning³⁷. It is unclear if this increased variability specifically corresponds to
377 increased exploration because both studies changed the sensory or the mechanical environment, which could have increased
378 variability by increasing unresolved sensorimotor noise. Further, according to our model, such increased variability comes with
379 a higher energetic cost at steady state² as well as potentially higher fall risk, so future work could use our model in concert with
380 targeted experiments to delineate how humans trade-off these competing objectives of exploration, energy, and stability.

381 Our model naturally predicts the various qualitative features of short timescale and long timescale responses to perturbations
382 without fitting to the adaptation phenomena being explained. This is in contrast to the single rate or dual rate or memory
383 of errors models of adaptation^{9,18,46}, which when applied to locomotor adaptation without including bipedal dynamics and
384 control, do require fits or specific assumptions to capture the direction of both the slow and the fast timescale transients. Here,
385 we predict the short timescale response to sudden perturbations as simply the response of the default stabilizing controller to
386 those perturbations, and this prediction obtains the correct direction or sign of the response without fits to the data it tries to
387 predict. For instance, our model naturally predicts that the immediate transient upon a split-belt perturbation or a leg mass
388 addition is negative step length asymmetry (Fig. 2-4). Similarly, we have shown that a substantial part of slow timescale motor
389 adaptation can be predicted by performance optimization, with energy consumption as the performance objective. This model
390 obtains the correct direction of the slow adaptation without any fits to the adaptation data. In contrast, in the traditional dual
391 rate or memory of errors adaptation models^{9,11,18}, the direction of slow adaptation is toward zeroing the error and, therefore, is
392 dictated by how error is defined. Thus, while descriptive models^{9,11,18} may be fit to short and long timescale transients in some
393 locomotor adaptation experiments, they do not make predictions of the transients from more primitive assumptions. In addition,
394 we have shown that some common ways of defining error, when coupled with locomotor dynamics, may result in predictions
395 that disagree with experiments.

396 Our accounting of savings and memory is complementary to previous work that have addressed savings or other related
397 phenomena via memory mechanisms centering on context inference for error-based learning or for performance improvement^{2,41,46,64}. These previous works did not consider the interaction of performance improvement and stabilizing control in a
398 complex task such as locomotion^{41,46,64}, as here, or when considering locomotion, did not consider locomotor dynamics and
399 control². Our memory model is also different from models that adapt the ‘error sensitivity’ (learning rate) of adaptation via
400 a memory of sensory errors⁹, which can capture savings in the form of faster adaptation rates, but is similar to other linear
401 time-invariant state-space models⁴⁶ in that neither model can capture savings in rate after a complete washout⁶⁵.

402 We have argued that predicting human locomotor adaptation phenomena may require the following functional components:
403 a stabilizing controller, an optimizing reinforcement learner, a gradient estimator, a memory mechanism, and possibly a module
404 that reduces sensory errors. Like all mathematical models of complex phenomena (famously in string theory⁶⁶), there may
405 be multiple realizability: the same architectural hypothesis can be expressed in different terms, grouping some components
406 together, dividing components into their sub-components, or have different realizations of similar function. No matter this
407 multiple realizability, we have shown that a necessary feature of locomotor adaptation is exploration in the neighborhood of
408 a stabilizing controller. Further, the framework implies the existence of a hierarchical separation of timescales of the model
409 components⁶⁷. Specifically, the step-to-step stabilizing controller has the fastest timescale, matching the timescale of the
410 bipedal dynamics to prevent falling; the timescale of gradient estimation must be slower than the step-to-step dynamics so
411 that the estimated gradient is reliable; finally, the timescale of the local reinforcement learner must be slower than the gradient
412 estimator, so that the learner does not change the parameters too quickly for the gradient estimate to be reliable. Human motor
413 learning proceeds over multiple timescales^{1,46}, and our approach thus provides a natural functional account of the hierarchy of
414 these timescales from the necessity of stable learning⁶⁷.

415 Our model of locomotor adaptation is hierarchical and modular. Evidence for the hypothesis of hierarchical and modular
416 motor control goes back to hundred year old experiments in which decerebrate cats produced coordinated repetitive movements
417 but not goal-directed movements⁶⁸. It is thought that fast timescale motor responses may be mediated in part by spinal circuits
418 while longer-timescale control, adaptation, and context-dependent responses may be achieved by interaction of the cerebellum
419 and motor-related areas of the cerebrum^{3,24,69,70}. In our model, we have separated the fast timescale stabilizing controller and
420 the slow timescale adaptation mechanisms into distinct interacting modules, so that damage to just the slow timescale adaptation

422 module in the model could still preserve the fast timescale stabilizing response. Such preservation of fast timescale response
423 to treadmill speed changes with degraded slow adaptation to a split-belt condition was found in participants with cerebellar
424 damage^{71,72}. Indeed, such studies have established that one locus of such slow timescale motor adaptation, especially involving
425 sensory recalibrations and internal model change, is the cerebellum^{3,11,12,71-74}. Thus, while our model is meant to be at the
426 Marr level 1 and 2 (computational and algorithmic levels)⁷⁵, it could inform interpretation of data on neural underpinnings.
427 Conversely, neural data may allow us to fine-tune our model architecture: for instance, modules in the model may contain
428 sub-modules responsible for distinct aspects of behavior which may be neurally dissociable (e.g., spatial and temporal slow
429 adaptation^{44,74}). Some studies have suggested preservation of ‘reinforcement learning’ despite cerebellar ataxia^{11,13,76}, but
430 such studies examined learning from explicit visual or auditory feedback, which is distinct from the implicit reinforcement
431 learning we have proposed for energy optimization.

432 Human motor control strategies in highly practiced and learned tasks tend to approximate optimal controllers⁷⁷, and here
433 we have provided an account for how humans gradually learn such optimal controllers in a novel environment. A related
434 learning paradigm is that the nervous system gradually learns an inverse model of the task dynamics from unsuccessful
435 trials, and then uses the inverse model to achieve the task⁷⁸. However, such inversion does not have a unique solution in
436 high-dimensional tasks such as locomotion: human bodies have infinitely many ways to solve a movement task²⁶ and thus must
437 usually optimize another performance objective to obtain a unique solution. Here, gradient descent of the stabilizing controller
438 implicitly accomplishes both the inversion and the optimization, as the resulting controller performs the task while optimizing
439 performance.

440 Our model demonstrates that a local exploration-based search strategy and a simple linear controller structure is sufficient
441 to describe the continuous adaptation of locomotion by human adults to changes to their body and their environment, starting
442 from a known default stabilizing controller, learned under normal conditions. Our approach may lend itself to comparison with
443 the recently popularized framework of deep reinforcement learning⁷⁹⁻⁸¹, which use more expressive controller approximations
444 (deep neural networks) with orders of magnitude more parameters. These methods do not assume initialization with a default
445 controller but instead employ highly exploratory search involving thousands of discrete walking episodes, often involve falling
446 and resetting the initial condition at the end of each episode. Thus, these learning methods operate in a different regime from
447 our model and are not aimed at explaining gradual human locomotor adaptation.

448 Most learning requires trial and error, but attempting to improve locomotion via simple trial and error without a stabilizing
449 controller as an inductive bias can result in falling or other learning instabilities. The stabilizing controller in our model allows
450 safe exploration and adaptation, and turning off the stabilizing feedback while the gait is adapted results in falls or at least
451 substantially degrades learning (Fig. 3). This shows that what control policy the learning acts on determines the effectiveness
452 and safety of the adaptation. We also found that a number of alternative choices can result in falling: prioritizing energy
453 optimization over the near future rather than over a longer time-horizon, too high a learning rate, and updating the gradient
454 estimate too quickly. We have posited the use of exploratory variability for reinforcement learning or optimization, as also
455 suggested in a few studies^{2,11,13,38}, including experimental evidence for the role of exploration in improving error-based
456 learning³⁸. It was not known how such exploration could be implemented to adapt while walking continuously, without ignoring
457 the locomotor dynamics, stability, and the continuous nature of locomotion (i.e., not treating each step as an independent
458 episode). Indeed, using simple trial and error to perform optimization, for instance, using an exploration-driven search
459 depending on just the previous step^{2,13}, works for episodic arm reaching but will result in falling or non-learning for walking
460 with continuous locomotor dynamics. Thus, here, we have put forth a framework for predicting how humans adapt their walking
461 to different conditions while continuing to be stable.

462 We have tested our model against a wide variety of adaptation studies, providing broad empirical support for the model’s
463 predictive ability. Future work can involve the design of targeted experiments to test the different components of this model
464 (e.g., performance objective, adaptation algorithm)⁸², as these components contain heretofore untested assumptions about
465 locomotor adaptation. Here, we have compared the predictive ability of performance objectives such as energy, symmetry,
466 and sensory prediction error, determining what each can predict when acting alone. Future experiments can systematically
467 manipulate the energy landscape, sensory feedback (e.g., vision), and unforeseen perturbations during adaptation to delineate
468 how these performance objectives are traded off by the human nervous system⁸³ — our model, which allows these adaptation
469 mechanisms to act simultaneously, can provide a framework for interpreting such experiments. Here, we have shown the
470 sufficiency of exploration-based gradient estimation and gradient descent with a fixed learning rate in predicting diverse
471 adaptation phenomena. Future experiments can compare the predictions of gradient descent versus alternative descent or
472 adaptation algorithms (e.g., gradient descent with momentum³⁹ or learning rate adaptation⁹) in long timescale trials that
473 either have gradually time-varying conditions or alternate between different conditions at various switching frequencies. Such
474 prospective experiments would allow us to characterize the relation between the adaptation direction in experiment and the
475 model-predicted gradient directions, thus helping to modify the model to capture a broader range of experiments. Future work
476 can also test the generality of our framework to other motor adaptation tasks^{41,77,84}, including the model’s ability to explain

477 savings, generalization, interference, non-learning, and other important phenomena; this application of our model to other
478 motor tasks will require appropriate modifications to the dynamical model and the default controller.

479 Our focus has been on capturing qualitative phenomena and we did not obtain a quantitative fit by minimizing the error
480 between model predictions and experiment. Consistent with this preference, we used a simple biped model with simplified
481 actuation, sensing, and default controller structure, which was sufficient for broad qualitative predictions but may limit ability
482 to produce detailed quantitative predictions; indeed, model simplicity may be a sound reason to not seek quantitative fits. While
483 we have captured a wide variety of experimental phenomena from diverse labs, future work could use a higher dimensional
484 musculoskeletal⁵⁶ and sensorimotor model and test it against other prior experimental data not considered here^{60,85-87} in
485 addition to the aforementioned prospective experiments. In these future studies, we would seek quantitative fits to many aspects
486 of the experimentally observed adaptation behavior (e.g., detailed kinematics, kinetics, energetics, variability), not just the time
487 course of one or two variables (as is typical) and without experiment-specific parameter tuning.

488 Model-based predictions of locomotor adaptation, such as enabled here, have potential applications to improving human-
489 machine interactions including robotic prostheses and exoskeletons, making such devices intrinsically more learnable or
490 devising protocols for accelerating their learning^{56,86,88}. Comparisons of learning in healthy and impaired human populations⁵³
491 using our modeling framework provides a means of identifying how distinct hypothesized modules of locomotor adaptation
492 may be affected, potentially informing targeted rehabilitation.

493 Methods

494 In this Methods section, we first describe the mathematical structure of each component of our modular and hierarchical
495 locomotor adaptation model (Fig. 1), how the components interact, and how this framework is applied to each task setting;
496 the human experiments are described at the end. Human participant research reported herein was approved by the Ohio State
497 University Institutional Review Board and all participants provided informed consent.

498 Stabilizing feedback controller

499 The mathematical biped model, approximating the human walker, is controlled on a step-to-step basis by a feedback controller.
500 The biped model and the stabilizing feedback controller^{16,26,31,89} are described in greater detail later in this *Methods* section
501 (see also *Supplementary Methods*). Here, we describe the general structure of the feedback controller necessary to understand
502 our modeling framework. The feedback controller is a function that relates the control variables u (e.g., forces and torques)
503 to the state variables s (positions and velocities). Here, the state s is a vector with as many elements as there are state
504 variables (n_{state} elements) and analogously u is a vector with n_{control} elements. The control variables have nominal values
505 u_{nominal} , sometimes referred to as a ‘feedforward’ term, which the biped uses in the absence of any perturbations at steady state.
506 Analogously, the state variables also have nominal values s_{nominal} in the absence of any external perturbations. Then, on step j ,
507 the control variables u_j are assumed to be related to the state s_j by the linear equation:

$$u_j = u_{\text{nominal}} + K \cdot (s_j - s_{\text{nominal}}), \quad (1)$$

508 where K is an $n_{\text{control}} \times n_{\text{state}}$ matrix of feedback gains. This equation 1 is equivalent to the simpler linear expression
509 $u_j = a + K \cdot s_j$, which has fewer parameters because the two vector variables u_{nominal} and s_{nominal} in equation 1 are replaced by
510 the one vector variable $a = u_{\text{nominal}} - K \cdot s_{\text{nominal}}$. This vector a may be considered the full ‘feedforward component’ of the
511 controller, in that it contains all terms that do not directly depend on current state. We use the version including u_{nominal} and
512 s_{nominal} in equation 1, in order to demonstrate the learner’s ability to automatically ignore redundant parameters. The linearity
513 of equation 1 is a simplifying assumption, justified by the ability of linear controllers to explain human step to step locomotor
514 control^{16,25,31,89} and its sufficiency for the adaptation phenomena explained by the framework here. The framework itself does
515 not rely on this assumption of linearity.

516 Local reinforcement learning for performance improvement

517 When faced with a novel situation, the reinforcement learner changes the parameters of the stabilizing controller to make progress
518 toward a defined objective, expressed as minimizing a scalar objective function or performance objective J evaluated over each
519 stride. The learnable parameters p characterizing the stabilizing controller include u_{nominal} , K , and s_{nominal} , i.e. the nominal
520 control and state values as well as the feedback gains. In this study, we only allow the nominal values $p = [u_{\text{nominal}}; s_{\text{nominal}}]$ to
521 change during learning. This is because there is a one-to-one mapping between these nominal or feedforward terms and the
522 overall gait kinematic changes we are trying to predict, so allowing the nominal values to change gives the model sufficient
523 flexibility to produce different kinematics. We keep the feedback gains K fixed, as the primary role of the feedback term
524 is to keep the system stable despite fast timescale perturbations away from the current gait pattern. Given the robustness
525 of the controller to substantial perturbations^{16,17}, this stabilizing role is satisfied by fixed feedback gains K . Indeed, as
526 assumed, we find that changing them is not necessary for the major phenomena discussed herein; allowing just the feedforward
527 term to change³ is sufficient (e.g., Fig. 2a-d). Allowing the feedback gains K to change may be necessary for even more
528 stability-challenging perturbations, where the robustness of the default controller no longer is sufficient — such changes to K
529 can be accomplished with the same framework but would require incorporating the locomotor task constraints explicitly into
530 the performance objective (e.g., not drifting off a finite treadmill, not falling, traveling a certain distance), as otherwise the
531 feedback gains may be chosen in a manner that makes the walker unstable. During learning, we allow the u_{nominal} and s_{nominal}
532 to change independently for the left and right steps, enabling adaptation to asymmetric conditions.

533 Fixing the overall structure of the controller during learning to that in equation 1 makes this initial controller structure an
534 inductive bias for learning; that is, it constrains exploration-based learning both by providing an initial condition and restricting
535 the space of controllers explored.

536 On each stride i (every two steps), we denote p_i to be the current best estimate of the controller parameters. We posit that
537 before encountering a novel condition, the body uses the previously learned controller for normal walking, which we have
538 characterized using data from normal walking^{16,31,89}. We term this the ‘default controller’ with parameters p_{default} , so that on
539 the first stride, the parameters are $p_1 = p_{\text{default}}$. Given the controller parameters p_i on stride i , the reinforcement learner chooses
540 the controller parameters for the next stride p_{i+1} as the sum of two terms: the old controller parameters from the previous stride
541 (p_i) and a small change along the negative of the gradient estimate of the performance objective:

$$p_{i+1} = p_i - \alpha_g(g_i), \quad (2)$$

542 where g_i is the current gradient estimate on the i^{th} stride (see equation 7 for how it is estimated) and α_g is a scalar learning rate
 543 for the gradient descent. Rather than executing the next stride using this new p_{i+1} , we posit that the nervous system uses a
 544 perturbed version \hat{p}_{i+1} :

$$\hat{p}_{i+1} = p_{i+1} + v_{i+1} \quad (3)$$

545 where v_{i+1} is an exploratory motor noise term, assumed to be multivariate Gaussian noise with standard deviation σ , uncorrelated
 546 across time. We posit that the exploratory noise v is intentionally generated by the nervous system, allowing it to estimate
 547 the local gradient of the performance objective J with respect to the parameters p , and more generally, build a local internal
 548 model of the system, serving as persistent excitation in the parlance of system identification^{90,91}. This exploration-based
 549 estimation of the gradient is in contrast with other simulation-based ways of estimating the gradient, for instance, algorithmic or
 550 automatic differentiation, also called backpropagation^{24,79}. In addition to this exploratory motor noise, there may be additional
 551 unavoidable sensory and motor noise that the nervous system cannot resolve, which we consider later separately^{92,93}. The
 552 proposed reinforcement learning procedure directly updates the parameters of the control policy via gradient descent, so it
 553 may be considered a variant of policy gradient reinforcement learning, where the gradient is estimated as below entirely from
 554 exploratory steps⁹⁴. Because the gradient is updated from limited and noisy data (see below), it is a stochastic gradient descent
 555 on the control policy. We term this learning ‘local’ because of its reliance on the information obtained via local exploration in
 556 the neighborhood of the controller to make gradual progress toward the optimum. In this formulation, the learnable parameters p
 557 are changed every stride, so that the effect of the left and the right step control on the performance objective can be experienced
 558 separately before being incorporated into the parameter change. This assumption of once-a-stride parameter change is not
 559 essential; the learning framework can be used with continuous phase-dependent control^{25,31} with more frequent or continuous
 560 updates of control parameters.

561 Asymptotic gradient estimate

562 Estimating the gradient of the performance objective J with respect to the parameters p is equivalent to building a local linear
 563 model relating changes in parameters p to changes in performance J . This can be understood by noting that a local linear
 564 model is the same as a first order Taylor series, and the gradient $\nabla_x f$ of a function $f(x)$ about x_0 appears as the coefficient of
 565 the variable x in this first order Taylor series as follows:

$$f(x) = f(x_0) + \nabla_x f \cdot (x - x_0) + \text{higher order terms} \approx \text{some constant} + \nabla_x f \cdot x. \quad (4)$$

566 The performance J on a given stride will not only depend on the controller parameters p , but the entire system trajectory,
 567 which is uniquely determined by the initial system state and the subsequent control actions given by p . So, we posit a linear
 568 model that includes dependence on both s_i and p_i . On stride i , if the initial state is s_i , the parameters are p_i , and the performance
 569 over that stride is J_i , a linear model relating these quantities is given by:

$$J_i = F s_i + G p_i + H. \quad (5)$$

570 Here, coefficient matrix G is the gradient of the performance J_i on the current stride with respect to the learning parameters p_i
 571 and the coefficient matrix F is the gradient with respect to initial state s_i . Building a linear model of J_i with respect to only p_i ,
 572 ignoring the dependence on state s_i can lead to incorrect gradient estimates and unstable learning.

573 Performing gradient descent using the matrix G as the gradient is equivalent to reducing the performance of a single stride
 574 J_i , without considering the long-term implications. Minimizing just the single-stride performance J_i may result in unrealistic
 575 optima for some performance objectives: turning off the actuators and falling may be optimal when only minimizing energy
 576 over one step. So, for non-transient tasks such as steady walking, we hypothesize that the human prioritizes the long term or
 577 steady state performance $J_\infty = \lim_{i \rightarrow \infty} J_i$. This asymptotic or long-horizon performance averages over the noise on any one
 578 stride.

579 To estimate the gradient with respect to long term performance, the nervous system needs to be able to predict the future.
 580 Thus, to predict the long-term consequences of the parameters p_i , we posit that the nervous system maintains an internal
 581 forward model of the dynamics, that is, how the initial state s_i and the parameters p_i for a stride affects the state at the end of
 582 the stride, equal to the initial state for the next stride s_{i+1} . This internal model of the dynamics is also assumed to be linear for
 583 simplicity:

$$s_{i+1} = A s_i + B p_i + C. \quad (6)$$

584 Given such an internal model of the dynamics, the nervous system can estimate the future consequences of parameter changes
 585 to the steady state (by effectively simulating the internal model to steady state) and thus infer the relevant gradient of J_∞ , given
 586 by:

$$g = \nabla J_\infty = G + F(I - A)^{-1}B, \quad (7)$$

587 where the first term G gives the gradient of the short term energy cost over one step, while the second term corrects for the fact
588 that the steady state value of s will be different from the current initial state s_i . This internal model framework also allows
589 the nervous system to minimize performance over an intermediate time horizon by computing and using the gradient of the
590 mean energy cost over the next few strides. We found that minimizing expected performance over just one or two strides into
591 the future can result in unstable learning for energy optimization. In conventional reinforcement learning⁹⁴, a discount factor
592 $0 < \gamma < 1$ is used to modify the function minimized to $\sum_{i=1}^{\infty} \gamma^{i-1} J_i$, which prioritizes near term performance and down-weights
593 performance in the future. We did not use such a discount factor here, but using $\gamma \approx 1$ is analogous to the asymptotic limit we
594 have chosen, and γ much less than one will give results similar to optimizing over just the next few strides.

595 We update the matrices A, B, C, F, G, H on each stride by estimating the linear model via ordinary least squares to best fit
596 the state, the action, and the performance (s_i, p_i, J_i) over a finite number of previous steps. We used a rolling estimate over 30
597 steps for all the results presented herein. This gradient estimator needs to have the property that relatively prioritizes recent
598 history⁹⁰, as otherwise, the gradient cannot adapt to novel locomotor situations in a timely manner. Using a finite history allows
599 rapid adaptation to sudden changes. Also, we use a linear internal model though the full biped dynamics are nonlinear; a linear
600 internal model is sufficient when adaptation is gradual and the model is constantly updated to be a good approximation about
601 the current operating point.

602 Learning happens as long as the gradient estimate, however computed, gives a reasonable descent direction on average —
603 that is, gives direction in which to change the control policy to lower the performance objective value. Operating on inaccurate
604 gradients can result in learning instabilities (distinct from instability in the movement dynamics), as can large gradient steps.
605 This learning instability can be prevented in two different ways. First, when the linear models in equations 5 and 6 are inaccurate,
606 as estimated by their residual being outside of the 95% confidence interval at steady state, the learning rate is set to zero. A
607 second approach to avoiding learning instability is a trust region approach, wherein the maximum gradient-based step-size is
608 limited to a fraction the exploratory noise. We tested both approaches and they give qualitatively similar results.

609 Forming motor memories and employing them when useful

610 We posit a modular memory unit to capture the fact that humans form and maintain memories of previously learned tasks⁴⁰, as
611 opposed to having to re-learn the tasks each time. First, we discuss our model of how such stored ‘motor memories’ are used,
612 and later in this section, we discuss how these motor memories are formed and updated based on experience.

613 Consider that the human had some past experience in the current task, and used controller parameters p_{memory} with
614 associated performance objective values J_{memory} . We posit that humans move toward this memory with some learning rate as
615 follows:

$$p_{i+1} = p_i + \alpha_g (-g_i) + \alpha_m (p_{\text{memory}} - p_i), \quad (8)$$

616 where $(p_{\text{memory}} - p_i)$ is the vector direction toward the memory and α_m is the rate at which memory is approached. We posit
617 that the controller parameters being learned move toward the memory only when $J_{\text{memory}} < J_{\text{current}}$, that is, when progressing
618 toward the memory improves the performance. Secondly, to ensure that progress toward memory does not destroy gradient
619 descent even if J_{memory} was inaccurately approximated, we posit that the learning rate α_m is modulated via a truncated cosine
620 tuning so that memory is used only when the direction toward memory does not oppose the direction of the negative gradient
621 (Fig. 1d). In *Supplementary Methods*, we elaborate mathematically on why this modulation of the rate toward memory is
622 necessary and sufficient to avoid convergence to a sub-optimal memory.

623 We conceive of a ‘motor memory’ as a pair of functions $F_p(\lambda)$ and $F_J(\lambda)$ that output the controller parameters $p_{\text{memory}} =$
624 $F_p(\lambda)$ and the corresponding performance objective value $J_{\text{memory}} = F_J(\lambda)$ respectively, given the task parameters λ (Fig.
625 1d). The task parameters λ could be continuous-valued, for instance, walking speed or assistance level of an exoskeleton,
626 or discrete-valued⁴¹, for instance, treadmill versus overground walking or presence versus absence of an exoskeleton. As a
627 simple example, the task parameter could be treadmill belt speed v_{belt} , and the stored motor memory functions $F_p(v_{\text{belt}})$ outputs
628 controller parameters for each walking speed and $F_J(v_{\text{belt}})$ outputs the corresponding performance objective value. In this case,
629 the nervous system could infer the belt speed v_{belt} from the sensory stream⁵⁵, by fusing proprioception (which can infer the
630 speed of head relative to foot, $v_{\text{head/foot}}$) and vision (which can sense the speed of head relative to lab, $v_{\text{head/lab}}$), so that the
631 belt speed is given by: $v_{\text{belt}} = v_{\text{foot/lab}} = v_{\text{head/lab}} - v_{\text{head/foot}}$. For simplicity, we assume that this task parameter inference is
632 independent of any potential perceptual recalibration^{22,42}, which is addressed separately in a later section on proprioceptive
633 realignment.

634 The memory functions F_p and F_J are built over time to approximate the best controllers learned during previous experiences
635 of similar tasks. We posit representations of motor memories via function approximation: in this manuscript, for simplicity,
636 the stored controller parameters p_{memory} are linear functions of the task parameters unless otherwise specified, anchored at a
637 nominal tied-belt condition. Such interpolating function approximations for memory are in contrast to discrete memories of
638 experiences without interpolation²: these two assumptions have different testable implications for generalization of learning.

639 The memory functions F_p and F_J have memory parameters μ , which determine the function approximation, for instance, the
640 slope and intercept of a linear functions $F_p(\lambda, \mu)$: here, we allow the slopes of the linear function to change to approximate new
641 experiences, while keeping the intercept at a nominal tied belt walking speed fixed. Analogous to our previous hypothesis that
642 the controller parameters are updated via gradient descent, we posit that these memory parameters are also updated via gradient
643 descent, so that the memory function better approximates controller parameters to be stored. That is, we posit that the nervous
644 system performs: $\mu_{i+1} = \mu_i - \alpha_{\text{mf}} \nabla_\mu L$, where L is a measure of how well the memory approximates the current controller p_i
645 and α_{mf} is the learning rate for memory formation; we used the root mean squared error over all controller parameters being
646 approximated. This memory update happens when the current controller p_i is better than what is already stored in the memory
647 i.e., when $J_{\text{current}} < J_{\text{memory}}$ or when the direction toward the memory is not a descent direction. This ensures that memory
648 formation and memory use are mutually exclusive (Fig. 1d).

649 **Minimal walking biped: dynamics, control, energy, and performance**

650 **Dynamics.** We consider a minimal model of bipedal walking (Supplementary Fig. 1a), consisting of a point-mass upper body
651 and simple legs that can change length and apply forces on the upper body^{26,54}. The total metabolic energy cost of walking for
652 this biped is defined as a weighted sum of the positive and negative work done by the stance legs on the upper body and the
653 work done to swing the legs forward^{54,95}. For this biped, the periodic energy-optimal walk on solid ground is the inverted
654 pendulum walking gait^{26,54,96}, in which the body vaults over the foot in a circular arc on each step (Supplementary Fig. 1b),
655 with the transition from one step to the next achieved via push-off by the trailing leg, followed by a heel-strike at the leading leg
656 (Supplementary Fig. 1c). We use this irreducibly minimal low-dimensional biped model^{26,54} to illustrate the predictive ability
657 of our modeling framework for simplicity and transparency. Further, we show that the simple model is sufficient for explaining
658 the major documented locomotor adaptation phenomena in the literature. The locomotor adaptation modeling framework herein
659 can be generalized to a more complex multibody multimuscle model of a human. The parameters of this biped model were not
660 fit to any data from the adaptation phenomena we seek to explain (see *Supplementary Methods*). When showing metabolic
661 energy cost transients for the model, we show two versions (e.g., in Fig. 2a), one that reflects average metabolic rate over each
662 stride and one that would be measured via indirect calorimetry, which is a low-pass filtered version of the stride-wise cost⁹⁷.

663 **Stabilizing feedback control.** The biped has two control variables for each leg, namely, step length and push-off magnitude
664 (Supplementary Fig. 1d), for a total of four discrete control actions per stride. These control variables are modulated to keep the
665 biped stable, despite external or internal noisy perturbations and despite a change in the mechanical environment e.g., walking
666 on a split-belt treadmill or with an exoskeleton. The controller keeps the biped stable despite large changes in the body and
667 environment, including external perturbations; this ability to be unaffected by unforeseen changes before any changes to the
668 controller parameters is called robustness, so that the controller is termed ‘robust’^{16,17,98}. The values of these control variables
669 on each step are decided by a discrete controller, as described below, derived from our prior human experiments on steady
670 walking^{16,17,31} without fitting any parameters to the data from the adaptation experiments we seek to explain. The body state s_i
671 at midstance at step i includes the forward position in the lab frame, the forward velocity in the belt and the lab frame, and
672 the running sum (i.e., discrete integral) of the forward position in the lab frame. The control variables u_i at step i are changed
673 by the following linear control rule as a function of the preceding midstance state s_i : $u_i = u_{\text{nominal}} + K \cdot (s_i - s_{\text{nominal}})$, where
674 K is a matrix of feedback gains^{16,31}. The velocity dependence of the control gains ensures that the walker doesn’t fall, the
675 position dependence promotes station-keeping^{17,31}, and integral dependence reduces error due to systematic changes in the
676 environment, for instance, changing the treadmill belt speeds or going from a tied to a split treadmill. These terms make the
677 controller a discrete PID controller (proportional-integral-derivative). The nominal periodic motion at each speed is governed
678 by the feedforward push-off and step length values, and these are selected so as to have the same speeds and step lengths as
679 a typical human (Supplementary Fig. 2). The default values for the control gain matrix K are then obtained by fitting the
680 dynamics of the model biped to the step to step map of normal human walking on a treadmill^{16,17,31,89}. Mathematical details
681 and parameter values are provided in the *Supplementary Methods*. All variables in equations and figures are non-dimensional,
682 unless otherwise mentioned: lengths normalized by leg length ℓ , masses normalized by total body mass, and time normalized
683 by $\sqrt{\ell/g}$, where g is acceleration due to gravity⁵⁴.

684 **Different locomotor task settings.** The biped model described above is expressive enough to capture the different task
685 settings for which we seek to model adaptation: walking with different exoskeleton assistance protocols, at varying belt speeds
686 (tied or split-belt), and with asymmetric leg masses. Here, we briefly describe how the different conditions are simulated by
687 changing the external environment and force it exerts on the biped. See *Supplementary Methods* for mathematical details.
688 The biped model described above allows the individual treadmill belt speeds to be changed as a function of time (Fig. 2a,c).
689 This generality is sufficient to simulate both split-belt and tied-belt treadmill walking conditions. The total metabolic cost
690 computed accounts for individual belt-speed changes because all components of the metabolic cost, namely, push-off work,
691 the heel-strike work, and the leg swing cost are computed by incorporating the relevant belt-speeds and effective leg masses.

692 For split-belt walking protocols, we usually use non-dimensional belt speeds of 0.5 for the fast belt and 0.25 or 0.3 for the
693 slow belt for many but not all computational results (Figs. 2a, 4, 5, 6, 7, 8): these walking speeds and their durations may be
694 different from precise experimental conditions but the qualitative features we illustrate are insensitive to such differences in
695 speeds chosen. We simulated exoskeletons as external devices in parallel to the leg that produce forward forces, or equivalently,
696 ankle torques (Figures 2d and 4e). Walking with periodic exoskeleton input used the perturbation as an additional input state in
697 the controller. For predicting adaptation to foot mass change (Fig. 2b), we incorporated the simplest leg swing dynamics: a
698 point-mass foot, propelled forward with an initial impulse and the foot mass coasting forward passively until heel-strike. For
699 the tied-belt walking, we used the belt speed as the task parameter; for split-belt studies, we used the individual belt speeds as
700 the task parameters; for the added leg mass study, we used the added leg mass as the task parameter. To track gait asymmetry,
701 we use the following two objectives of left-right asymmetry⁴, namely step length asymmetry and step time asymmetry, defined
702 as follows:

$$\text{step length asymmetry} = \frac{D_{\text{fast}} - D_{\text{slow}}}{D_{\text{fast}} + D_{\text{slow}}} \text{ and step time asymmetry} = \frac{T_{\text{fast}} - T_{\text{slow}}}{T_{\text{fast}} + T_{\text{slow}}}, \quad (9)$$

703 where the fast and the slow step lengths (D_{fast} and D_{slow}) are defined at heel strike as in Supplementary Fig. 1e and the step
704 times T_{fast} and T_{slow} are the stance times when on the fast and slow belts respectively. We use analogous objectives when the
705 biped walks with an asymmetric foot mass. There can be other ways of quantifying asymmetry and we chose asymmetry
706 objectives that are commonly used to empirically track adaptation^{4, 5, 45}. A zero value indicates symmetry with respect to these
707 measures, but does not imply perfect left-right symmetry of the entire motion.

708 All computational work was performed in MATLAB (version 2022a). See Supplementary Methods and our codebase
709 implementing these simulations, *LocAd*³⁰, shared via a public repository. Data from prior manuscripts^{5, 6, 8, 18, 20, 28, 45, 48, 51, 99, 100}
710 are plotted in Figures 2, 6a, and 7b and Supplementary Figures 2, 4, 6, as cited in place, to illustrate how model-based
711 predictions agree qualitatively with experimental results in prior studies.

712 Alternative to performance optimization: Comparison with proprioceptive realignment

713 Experimental evidence during split-belt adaptation suggests some recalibration of proprioception by the two legs⁴² and has
714 been argued to be at least partially responsible for kinematic adaptation^{22, 42} based on correlation of timescales between such
715 realignment and adaptation. No mathematical model been been previously proposed for how such realignment may happen.
716 Without such a mathematical model, it is impossible to know whether the direction of adaptation due to such realignment will
717 be consistent with or opposing that observed in experiment. Here, we first present such a mathematical model and then test the
718 extent to which it explains adaptation on a split-belt treadmill. We implement this proprioceptive realignment as a sensory
719 recalibration of the input to the stabilizing controller, replacing the gradient-based reinforcement learner (Fig. 9a-b).

720 Recalibration takes place when there is substantial conflict between what is expected by the nervous system and what is
721 sensed¹¹. The key missing hypothesis in extending such sensory recalibration to locomotor adaptation lies in the question:
722 what error is the nervous system using to drive recalibration during locomotion? We hypothesize that, given the typical walking
723 experienced in daily life, the nervous system expects the two legs to be on a common surface: this expectation results in a
724 sensory conflict on a split-belt treadmill with both feet experiencing unequal belt speeds.

725 When the walking surface has fixed speed and the visual environment is uniform, the walking speed can be estimated by the
726 nervous system by two sensory modalities¹⁰¹: vision (based on visual flow) and proprioception (by integrating joint angles
727 and angle rates from muscle spindles and Golgi tendon organs). On a treadmill in a lab, vision has information about how the
728 head moves with respect to the lab, so we identify the visual speed with $v_{\text{body/lab}}$. Proprioception has information about how
729 fast the body parts move relative to the stance foot on the belt, so we identify proprioception with $v_{\text{body/belt}}$. Thus, the body
730 has information to implicitly estimate the belt speed via the following equation: $v_{\text{belt/lab}} = v_{\text{body/lab}} - v_{\text{body/belt}}$. On a split-belt
731 treadmill, all these speeds will be belt-specific, e.g., $v_{\text{belt,1/lab}}$ and $v_{\text{belt,2/lab}}$. The expectation that both legs contact a common
732 surface can be expressed as the equality of these individual belt speeds: $v_{\text{belt,1/lab}} = v_{\text{belt,2/lab}}$. We posit that deviations from this
733 equality result in slow recalibration. Consistent with much of the arm reaching literature, we recalibrate only the proprioceptive
734 sense, hence the term proprioceptive realignment.

735 Say, $\bar{v}_{\text{body/belt,1}}$ and $\bar{v}_{\text{body/belt,2}}$ are the proprioceptively obtained sensory information from the two legs without recalibration,
736 and $\hat{v}_{\text{body/belt,1}}$ and $\hat{v}_{\text{body/belt,2}}$ are the recalibrated versions. The two versions are related by:

$$\hat{v}_{\text{body/belt,1}} = \bar{v}_{\text{body/belt,1}} - \Delta v_1 \text{ and } \hat{v}_{\text{body/belt,2}} = \bar{v}_{\text{body/belt,2}} - \Delta v_2, \quad (10)$$

737 where Δv_1 and Δv_2 are the recalibrative corrections. We describe this recalibration as happening via a state observer with two
738 timescales: a fast timescale process estimating a common belt speed \hat{v}_{common} using proprioceptive information from both legs
739 and a slow timescale process estimating the recalibrative corrections Δv_1 and Δv_2 for each leg separately. The common belt

740 speed estimate is updated every step j via a state observer as follows:

$$\hat{v}_{\text{common}}(j+1) = \hat{v}_{\text{common}}(j) + a_{\text{common}} (\bar{v}_{\text{body/lab}}(j) - \bar{v}_{\text{body/belt,k}}(j) - \hat{v}_{\text{common}}(j)) \quad (11)$$

741 where k equals 1 or 2 for odd and even step number given by j , respectively, and a_{common} is a rate constant proportional to the time
742 spent on each step – but we treat as constant for simplicity. This equation results in convergence of \hat{v}_{common} to the average belt
743 speed. The recalibration Δv_k is the current estimated perturbation of the individual belt speed from the estimated common speed
744 \hat{v}_{common} . This recalibration is updated on every stride i as: $\Delta v_k(i+1) = \Delta v_k(i) + a_{\Delta} (\bar{v}_{\text{body/lab}} - \bar{v}_{\text{belt,k/lab}} - \hat{v}_{\text{common}} - \Delta v_k(i))$.
745 Here, the rate constant a_{Δ} is much smaller than a_{common} , reflecting the slower timescale at which the perturbation estimate
746 $\Delta \hat{v}_k$ is updated. Here, \hat{v}_1 is updated on odd steps and \hat{v}_2 is updated on even steps. This perturbation estimate Δv_k eventually
747 converges to the deviation of the actual belt speed from the common speed. These state observer equations for recalibration
748 are similar to estimating the belt speed via a state estimator reflecting an expectation that tied-belt changes are much more
749 likely than split-belt changes, modeled by the noise covariance matrix for belt speed changes having large diagonal elements
750 (governing co-variation of belt speeds) and small off-diagonal elements (governing belt speed differences). Further, while we
751 have introduced the latent variables v_{common} and Δv_k in the above description, the recalibration equations can be written without
752 such latent variables. The recalibrated proprioceptive information ($\hat{v}_{\text{body/belt,1}}$ and $\hat{v}_{\text{body/belt,2}}$) is used in the stabilizing controller
753 instead of the direct proprioception. In the Results, we show effects of 50% and 100% recalibration: 100% corresponds to
754 using the full correction Δv_k and 50% uses 0.5 Δv_k in the recalibration equation 10.

755 Alternative to energy minimization: Comparison with reducing kinematic task error

756 Minimizing kinematic task error first requires defining what the desired or expected kinematics are. To define this, we first
757 note that slow timescale error minimization is not thought to underlie tied-belt walking adaptation, or at least the timescales of
758 adaptation to tied-belt speed changes are much faster than for split-belt adaptation²⁸. So, we posit that the nervous system
759 treats tied-belt walking — or walking on the same surface with both legs — as the normal state of affairs, basing the desired
760 kinematics on an implicit assumption of tied-belt walking. The nervous system estimates the common belt speed \hat{v}_{common} as in
761 the previous section, using visual flow and proprioception from both legs (see eq. 11 and Fig. 8b). This common belt speed
762 \hat{v}_{common} is then used to make a prediction for the body midstance state \hat{s}_{common} based on memory, which is compared with
763 actual sensory information \bar{s} to compute the task error $E = \hat{s}_{\text{common}} - \bar{s}$.

764 In simple tasks such as arm reaching, where both the error and the action is one-dimensional, it is possible to reduce error
765 via a simple ‘error-based learning model’ with a single or dual rate process⁴⁶ or via learning rate adaptation⁹. However, in
766 tasks such as walking in a novel environment, because body state and the number of actuators is high-dimensional, the nervous
767 system may not have a priori inverse model to produce the motor actions that reduce the error. So, a simple one-dimensional
768 error based learning model is not appropriate. We instead model the error reduction as proceeding analogous to energy reduction
769 via gradient descent using exploratory variability to estimate gradients, as a special case of the framework in Fig. 1. The
770 kinematic task error being minimized may also be considered a kind of sensory prediction error, as the error from the kinematic
771 state predicted or expected by the nervous system given the belt speed estimate.

772 Interaction with explicit control

773 The mechanisms proposed herein are for implicit adaptation, but these mechanisms allow for explicit (conscious) control acting
774 in parallel to implicit adaptation. We show how our model can be extended to interact with explicit input by implementing
775 an visually-informed explicit control module for the reduction of step length asymmetry¹⁰. On each step, the explicit control
776 module outputs a correction to the desired step length proportional to the step length asymmetry on the previous stride, with the
777 intention of reducing the step length asymmetry on the current step. This output from the explicit control module is added to
778 the desired step length output from the implicit adaptation module (the default adaptation mechanisms here), so that the net
779 total control input is used by the stabilizing controller. The additive and parallel nature of the implicit and explicit modules are
780 as proposed for explicit control in arm reaching studies²³. The architecture of the interaction between the implicit adaptation
781 and explicit control is such that the implicit module is only aware of its own output and not that of the explicit module; thus, the
782 implicit module optimizes the objective with respect to its own output.

783 Prospective experiments

784 The computational model we put forth here can be used to design prospective experiments, augmenting experimenter intuition.
785 Here, we conducted two model-guided experiments to test predictions of the model that are surprising when compared to the
786 existing literature: (1) on the effect of environment noise on locomotor adaptation, and (2) on the effect of an immediately
787 preceding counter-perturbation on a subsequent adaptation.

788 Twenty five participants (19 male, 6 female, self-reported sex, age 21.9 ± 3 years, mean \pm s.d.) participated with informed
789 consent and the experiments were approved by the Ohio State University IRB. Participants were assigned randomly into two

790 groups: sixteen participants performed experiment 1 (12 male, 4 female, age 21.7 ± 3 years) and nine participants (6 male, 3
791 female, age 22.3 ± 3 years) performed experiment 2. Both experiments involved walking on a split-belt treadmill (Bertec Inc.),
792 with the details of the protocol provided below. Foot movement was tracked via a Vicon T20 motion capture system (Vicon
793 Nexus 1.x). Sex or age were not used as an explanatory variable in any analysis, as the computational model tested does not
794 include such variables.

795 Experiment 1 was designed to test the model prediction that when the belt noise level was sufficiently high, learning can
796 be degraded, which is surprising relative to a prior finding that a modest level of belt noise can slightly enhance learning
797 as measured by after-effects²⁰. For this experiment, the participants were sub-divided into two groups of eight: one group
798 performed a no-noise abrupt protocol (Fig. 7a), in which participants started walking under tied-belt conditions at 0.9 m/s,
799 then adapted to split-belt condition of 0.6 m/s and 1.2 m/s kept constant for 10 minutes, followed by three minutes of tied-belt
800 walking at 0.6 m/s; the second group had an identical protocol except the split-belt condition involved continuously changing
801 belt speed for just the fast belt, fluctuating in a piecewise linear manner with zero mean and 0.2 m/s standard deviation (normally
802 distributed). The consecutive grid points of the piecewise linear noise were separated by 1.2 seconds, roughly equal to a stride
803 period, so that the noise value was different two strides apart (the noise in²⁰ was changed every 3 seconds, and thus had greater
804 temporal correlation); speed changes had 0.1-0.2 m/s² accelerations. The noise standard deviation was set at a lower level in
805 simulation (0.04 m/s) to ensure stability. The post-adaptation after-effect in step length asymmetry after baseline subtraction,
806 averaged over the first 8 strides (about 10 seconds) was used as a measure of adaptation similar to prior work²⁰. We compared
807 these after-effects between the noise and no-noise case, testing the hypothesis that the noise case has lower after-effects.

808 Experiment 2 was designed to test the model prediction regarding savings, specifically whether experiencing a counter
809 perturbation B beforehand, interferes with adaptation to perturbation A. Previous experiment had found that if B and A were
810 separated by a washout period, the adaptation to A was not significantly affected compared to not having experienced B. Our
811 model had a distinct prediction for when A immediately followed B, without a washout period W. So, participants performed
812 this experimental protocol T-B-A (Fig. 6) in which 4 minutes of walking on a tied-belt at 0.9 m/s (T) was followed by a split-belt
813 condition with belt speeds of 0.6 and 1.2 m/s for 10 minutes (B), immediately followed by the opposite split-belt condition 1.2
814 and 0.6 m/s for 10 minutes. Equivalent to comparing the A of protocols T-A and T-B-A by symmetry, we compared the initial
815 transient and the time-constant of the two adaptation periods B and A in T-B-A: the B of T-B-A was without prior split-belt
816 experience and the A of T-B-A is the adaptation phase just after a counter-perturbation.

817 **Data availability.** The experimental data generated in this study have been deposited in the Dryad database with DOI:
818 10.5061/dryad.kh18932gq. Source data are provided with this paper. Other human experimental data or results referred to
819 herein are available in previously published manuscripts^{5,6,8,18,20,28,45,48,51,52,99,100}.

820 **Code availability.** Code associated with this paper, *LocAd*³⁰, is available at: <https://github.com/SeethapathiLab/LocAd>

822 References

- 823 1. Day, K. A., Leech, K. A., Roemmich, R. T. & Bastian, A. J. Accelerating locomotor savings in learning: compressing
824 four training days to one. *J. Neurophys.* **119**, 2100–2113 (2018).
- 825 2. Selinger, J. C., Wong, J. D., Simha, S. N. & Donelan, J. M. How humans initiate energy optimization and converge on
826 their optimal gaits. *J. Exp. Biol.* **222**, jeb198234 (2019).
- 827 3. Bastian, A. J. Learning to predict the future: the cerebellum adapts feedforward movement control. *Curr. Opin. Neurobiol.*
828 **16**, 645–649 (2006).
- 829 4. Reisman, D. S., Block, H. J. & Bastian, A. J. Interlimb coordination during locomotion: what can be adapted and stored?
830 *J. Neurophysiol.* **94**, 2403–2415 (2005).
- 831 5. Noble, J. W. & Prentice, S. D. Adaptation to unilateral change in lower limb mechanical properties during human walking.
832 *Exp. Brain Res.* **169**, 482–495 (2006).
- 833 6. Finley, J., Bastian, A. & Gottschall, J. Learning to be economical: the energy cost of walking tracks motor adaptation. *J.*
834 *Physiol.* **591**, 1081–1095 (2013).
- 835 7. Sánchez, N., Simha, S. N., Donelan, J. M. & Finley, J. M. Taking advantage of external mechanical work to reduce
836 metabolic cost: The mechanics and energetics of split-belt treadmill walking. *J. Physiol.* **597**, 4053–4068 (2019).
- 837 8. Selinger, J. C., O Connor, S. M., Wong, J. D. & Donelan, J. M. Humans can continuously optimize energetic cost during
838 walking. *Curr. Biol.* **25**, 2452–2456 (2015).
- 839 9. Herzfeld, D. J., Vaswani, P. A., Marko, M. K. & Shadmehr, R. A memory of errors in sensorimotor learning. *Science* **345**,
840 1349–1353 (2014).
- 841 10. Roemmich, R. T., Long, A. W. & Bastian, A. J. Seeing the errors you feel enhances locomotor performance but not
842 learning. *Curr. biology* **26**, 2707–2716 (2016).
- 843 11. Izawa, J. & Shadmehr, R. Learning from sensory and reward prediction errors during motor adaptation. *PLoS computational biology* **7**, e1002012 (2011).
- 844 12. Tseng, Y.-w., Diedrichsen, J., Krakauer, J. W., Shadmehr, R. & Bastian, A. J. Sensory prediction errors drive cerebellum-
845 dependent adaptation of reaching. *J. neurophysiology* **98**, 54–62 (2007).
- 846 13. Therrien, A. S., Wolpert, D. M. & Bastian, A. J. Effective reinforcement learning following cerebellar damage requires a
847 balance between exploration and motor noise. *Brain* **139**, 101–114 (2016).
- 848 14. Hof, A., Vermerris, S. & Gjaltema, W. Balance responses to lateral perturbations in human treadmill walking. *J Exp Biol*
849 **213**, 2655–2664 (2010).
- 850 15. Seyfarth, A., Geyer, H. & Herr, H. Swing-leg retraction: a simple control model for stable running. *J Exp Biol* **206**,
851 2547–2555 (2003).
- 852 16. Joshi, V. & Srinivasan, M. A controller for walking derived from how humans recover from perturbations. *J. Roy. Soc.*
853 *Interface* **16**, 20190027 (2019).
- 854 17. Seethapathi, N. & Srinivasan, M. Step-to-step variations in human running reveal how humans run without falling. *ELife*
855 **8**, e38371 (2019).
- 856 18. Roemmich, R. T. & Bastian, A. J. Two ways to save a newly learned motor pattern. *J. Neurophys.* **113**, 3519–3530 (2015).
- 857 19. Simha, S. N., Wong, J. D., Selinger, J. C., Abram, S. J. & Donelan, J. M. Increasing the gradient of energetic cost does
858 not initiate adaptation in human walking. *J. Neurophysiol.* **126**, 440–450 (2021).
- 859 20. Torres-Oviedo, G. & Bastian, A. J. Natural error patterns enable transfer of motor learning to novel contexts. *J.*
860 *Neurophysiol.* **107**, 346–356 (2012).
- 861 21. Long, A. W., Roemmich, R. T. & Bastian, A. J. Blocking trial-by-trial error correction does not interfere with motor
862 learning in human walking. *J. neurophysiology* **115**, 2341–2348 (2016).
- 863 22. Rossi, C., Bastian, A. J. & Therrien, A. S. Mechanisms of proprioceptive realignment in human motor learning. *Curr.*
864 *Opin. Physiol.* **20**, 186–197 (2021).
- 865 23. Taylor, J. A. & Ivry, R. B. Flexible cognitive strategies during motor learning. *PLoS computational biology* **7**, e1001096
866 (2011).
- 867 24. Fujiki, S. *et al.* Adaptation mechanism of interlimb coordination in human split-belt treadmill walking through learning
868 of foot contact timing: a robotics study. *J. Royal Soc. Interface* **12**, 20150542 (2015).

870 25. Seethapathi, N. *Transients, Variability, Stability and Energy in Human Locomotion*. Ph.D. thesis, The Ohio State
871 University (2018).

872 26. Srinivasan, M. & Ruina, A. Computer optimization of a minimal biped model discovers walking and running. *Nature*
873 **439**, 72–75 (2006).

874 27. Simha, S. N., Wong, J. D., Selinger, J. C., Abram, S. J. & Donelan, J. M. Increasing the gradient of energetic cost does
875 not initiate adaptation in human walking. *bioRxiv* (2020).

876 28. Pagliara, R., Snaterse, M. & Donelan, J. M. Fast and slow processes underlie the selection of both step frequency and
877 walking speed. *J. Exp. Biol.* **217**, 2939–2946 (2014).

878 29. Ahn, J. & Hogan, N. A simple state-determined model reproduces entrainment and phase-locking of human walking.
879 *PloS one* **7**, e47963 (2012).

880 30. Seethapathi, N., Clark, B. & Srinivasan, M. Locad: Code for ‘exploration-based learning of a stabilizing controller
881 predicts locomotor adaptation’. <https://github.com/SeethapathiLab/LocAd> (2024).

882 31. Wang, Y. & Srinivasan, M. Stepping in the direction of the fall: the next foot placement can be predicted from current
883 upper body state in steady-state walking. *Biol. Lett.* **10**, 20140405 (2014).

884 32. Ralston, H. J. Energy-speed relation and optimal speed during level walking. *Int Z angew Physiol einschl Arbeitsphysiol*
885 **17**, 277–283 (1958).

886 33. Zarrugh, M., Todd, F. & Ralston, H. Optimization of energy expenditure during level walking. *Eur. J. Appl. Physiol.
887 Occup. Physiol.* **33**, 293–306 (1974).

888 34. Long, L. L. & Srinivasan, M. Walking, running, and resting under time, distance, and average speed constraints: optimality
889 of walk–run–rest mixtures. *J. R. Soc. Interface* **10**, 20120980 (2013).

890 35. Seethapathi, N. & Srinivasan, M. The metabolic cost of changing walking speeds is significant, implies lower optimal
891 speeds for shorter distances, and increases daily energy estimates. *Biol. Lett.* **11**, 20150486 (2015).

892 36. Bertram, J. & Ruina, A. Multiple walking speed–frequency relations are predicted by constrained optimization. *J. Theor.
893 Biol.* **209**, 445–453 (2001).

894 37. Torres-Oviedo, G. & Bastian, A. J. Seeing is believing: effects of visual contextual cues on learning and transfer of
895 locomotor adaptation. *J. Neurosci.* **30**, 17015–17022 (2010).

896 38. Wu, H. G., Miyamoto, Y. R., Castro, L. N. G., Ölveczky, B. P. & Smith, M. A. Temporal structure of motor variability is
897 dynamically regulated and predicts motor learning ability. *Nat. neuroscience* **17**, 312–321 (2014).

898 39. Sutton, R. S. & Barto, A. G. *Reinforcement learning: An introduction* (MIT press, 2018).

899 40. Brashers-Krug, T., Shadmehr, R. & Bizzi, E. Consolidation in human motor memory. *Nature* **382**, 252–255 (1996).

900 41. Heald, J. B., Lengyel, M. & Wolpert, D. M. Contextual inference underlies the learning of sensorimotor repertoires.
901 *Nature* **600**, 489–493 (2021).

902 42. Vazquez, A., Statton, M. A., Busgang, S. A. & Bastian, A. J. Split-belt walking adaptation recalibrates sensorimotor
903 estimates of leg speed but not position or force. *J. neurophysiology* **114**, 3255–3267 (2015).

904 43. Kluzik, J., Diedrichsen, J., Shadmehr, R. & Bastian, A. J. Reach adaptation: what determines whether we learn an internal
905 model of the tool or adapt the model of our arm? *J. neurophysiology* **100**, 1455–1464 (2008).

906 44. Choi, J. T., Vining, E. P., Reisman, D. S. & Bastian, A. J. Walking flexibility after hemispherectomy: split-belt treadmill
907 adaptation and feedback control. *Brain* **132**, 722–733 (2008).

908 45. Sánchez, N., Simha, S. N., Donelan, J. M. & Finley, J. M. Using asymmetry to your advantage: learning to acquire and
909 accept external assistance during prolonged split-belt walking. *J. Neurophysiol.* **125**, 344–357 (2021).

910 46. Smith, M. A., Ghazizadeh, A. & Shadmehr, R. Interacting adaptive processes with different timescales underlie short-term
911 motor learning. *PLoS Biol* **4**, e179 (2006).

912 47. Stenum, J. & Choi, J. T. Step time asymmetry but not step length asymmetry is adapted to optimize energy cost of
913 split-belt treadmill walking. *The J. Physiol.* **598**, 4063–4078 (2020).

914 48. Ochoa, J., Sternad, D. & Hogan, N. Treadmill vs. overground walking: different response to physical interaction. *J.
915 Neurophysiol.* **118**, 2089–2102 (2017).

916 49. Buurke, T. J., Lamoth, C. J., van der Woude, L. H. & den Otter, R. Handrail holding during treadmill walking reduces
917 locomotor learning in able-bodied persons. *IEEE Transactions on Neural Syst. Rehabil. Eng.* **27**, 1753–1759 (2019).

918 50. Park, S. & Finley, J. M. Manual stabilization reveals a transient role for balance control during locomotor adaptation. *J. Neurophysiol.* **128**, 808–818 (2022).

919 51. Malone, L. A., Vasudevan, E. V. & Bastian, A. J. Motor adaptation training for faster relearning. *J. Neurosci.* **31**, 920 15136–15143 (2011).

921 52. Leech, K. A., Roemmich, R. T. & Bastian, A. J. Creating flexible motor memories in human walking. *Sci. Rep.* **8**, 1–10 922 (2018).

923 53. Lam, J. *et al.* Impaired implicit learning and feedback processing after stroke. *Neurosci.* **314**, 116–124 (2016).

924 54. Srinivasan, M. Fifteen observations on the structure of energy-minimizing gaits in many simple biped models. *J. R. Soc. 925 Interface* **8**, 74–98 (2011).

926 55. Srinivasan, M. Optimal speeds for walking and running, and walking on a moving walkway. *Chaos* **19**, 026112 (2009).

927 56. Handford, M. L. & Srinivasan, M. Robotic lower limb prosthesis design through simultaneous computer optimizations of 928 human and prosthesis costs. *Sci. Rep.* **6**, 19983 (2016).

929 57. Henriques, D. Y. & Cressman, E. K. Visuomotor adaptation and proprioceptive recalibration. *J. motor behavior* **44**, 930 435–444 (2012).

931 58. Tsay, J. S., Kim, H., Haith, A. M. & Ivry, R. B. Understanding implicit sensorimotor adaptation as a process of 932 proprioceptive re-alignment. *Elife* **11**, e76639 (2022).

933 59. Reisman, D., Wityk, R., Silver, K. & Bastian, A. Locomotor adaptation on a split-belt treadmill can improve walking 934 symmetry post-stroke. *Brain* **130**, 1861–1872 (2007).

935 60. Leech, K. A., Day, K. A., Roemmich, R. T. & Bastian, A. J. Movement and perception recalibrate differently across 936 multiple days of locomotor learning. *J. neurophysiology* **120**, 2130–2137 (2018).

937 61. Friston, K. The free-energy principle: a unified brain theory? *Nat. reviews neuroscience* **11**, 127–138 (2010).

938 62. Abram, S. J., Selinger, J. C. & Donelan, J. M. Energy optimization is a major objective in the real-time control of step 939 width in human walking. *J. biomechanics* **91**, 85–91 (2019).

940 63. Wong, J. D., Selinger, J. C. & Donelan, J. M. Is natural variability in gait sufficient to initiate spontaneous energy 941 optimization in human walking? *J. neurophysiology* **121**, 1848–1855 (2019).

942 64. Pekny, S. E., Criscimagna-Hemminger, S. E. & Shadmehr, R. Protection and expression of human motor memories. *J. 943 Neurosci.* **31**, 13829–13839 (2011).

944 65. Zarahn, E., Weston, G. D., Liang, J., Mazzoni, P. & Krakauer, J. W. Explaining savings for visuomotor adaptation: linear 945 time-invariant state-space models are not sufficient. *J. neurophysiology* **100**, 2537–2548 (2008).

946 66. Witten, E. String theory dynamics in various dimensions. *Nucl. Phys. B* **443**, 85–126 (1995).

947 67. Anderson, B. D. Failures of adaptive control theory and their resolution. *Comm. Info. Sys.* **5**, 1–20 (2005).

948 68. Hamilton, A. & Grafton, S. T. The motor hierarchy: from kinematics to goals and intentions. *Sensorimotor foundations 949 higher cognition* **22**, 381–408 (2007).

950 69. Armstrong, D. Supraspinal contributions to the initiation and control of locomotion in the cat. *Prog. neurobiology* **26**, 951 273–361 (1986).

952 70. Drew, T., Prentice, S. & Schepens, B. Cortical and brainstem control of locomotion. *Prog. brain research* **143**, 251–261 953 (2004).

954 71. Statton, M. A., Vazquez, A., Morton, S. M., Vasudevan, E. V. & Bastian, A. J. Making sense of cerebellar contributions to 955 perceptual and motor adaptation. *The Cerebellum* **17**, 111–121 (2018).

956 72. Morton, S. M. & Bastian, A. J. Cerebellar contributions to locomotor adaptations during splitbelt treadmill walking. *J. 957 Neurosci.* **26**, 9107–9116 (2006).

958 73. Bastian, A. J. Moving, sensing and learning with cerebellar damage. *Curr. opinion neurobiology* **21**, 596–601 (2011).

959 74. Darmohray, D. M., Jacobs, J. R., Marques, H. G. & Carey, M. R. Spatial and temporal locomotor learning in mouse 960 cerebellum. *Neuron* **102**, 217–231 (2019).

961 75. Marr, D. *Vision: A computational investigation into the human representation and processing of visual information* (MIT 962 press, 2010).

963

964 76. Therrien, A. S., Statton, M. A. & Bastian, A. J. Reinforcement signaling can be used to reduce elements of cerebellar
965 reaching ataxia. *The Cerebellum* **20**, 62–73 (2021).

966 77. Todorov, E. & Jordan, M. I. Optimal feedback control as a theory of motor coordination. *Nat. Neurosci.* **5**, 1226–1235
967 (2002).

968 78. Jordan, M. I. & Rumelhart, D. E. Forward models: Supervised learning with a distal teacher. *Cog. Sci.* **16**, 307–354
969 (1992).

970 79. Peng, X. B., Berseth, G., Yin, K. & Van De Panne, M. Deeploco: Dynamic locomotion skills using hierarchical deep
971 reinforcement learning. *ACM Trans. Graph. (TOG)* **36**, 1–13 (2017).

972 80. Kidziński, Ł. *et al.* Learning to run challenge solutions: Adapting reinforcement learning methods for neuromusculoskeletal
973 environments. In *The NIPS'17 Competition: Building Intelligent Systems*, 121–153 (Springer, 2018).

974 81. Xie, Z., Berseth, G., Clary, P., Hurst, J. & van de Panne, M. Feedback control for cassie with deep reinforcement learning.
975 In *2018 IEEE/RSJ International Conference on Intelligent Robots and Systems (IROS)*, 1241–1246 (IEEE, 2018).

976 82. Ajemian, R. & Hogan, N. Experimenting with theoretical motor neuroscience. *J. motor behavior* **42**, 333–342 (2010).

977 83. Cashaback, J. G., McGregor, H. R., Mohatarem, A. & Gribble, P. L. Dissociating error-based and reinforcement-based
978 loss functions during sensorimotor learning. *PLoS computational biology* **13**, e1005623 (2017).

979 84. Albert, S. T. *et al.* Competition between parallel sensorimotor learning systems. *Elife* **11**, e65361 (2022).

980 85. Sombrio, C. J., Calvert, J. S. & Torres-Oviedo, G. Large propulsion demands increase locomotor adaptation at the expense
981 of step length symmetry. *Front. physiology* **10**, 60 (2019).

982 86. Zhang, J. *et al.* Human-in-the-loop optimization of exoskeleton assistance during walking. *Science* **356**, 1280–1284
983 (2017).

984 87. Vasudevan, E. V. & Bastian, A. J. Split-belt treadmill adaptation shows different functional networks for fast and slow
985 human walking. *J. neurophysiology* **103**, 183–191 (2010).

986 88. Gordon, K. E. & Ferris, D. P. Learning to walk with a robotic ankle exoskeleton. *J. Biomech.* **40**, 2636–2644 (2007).

987 89. Perry, J. A. & Srinivasan, M. Walking with wider steps changes foot placement control, increases kinematic variability
988 and does not improve linear stability. *Roy. Soc. Open Sci.* **4**, 160627 (2017).

989 90. Goodwin, G. C. & Sin, K. S. *Adaptive filtering prediction and control* (Courier Corporation, 2014).

990 91. Herzfeld, D. J. & Shadmehr, R. Motor variability is not noise, but grist for the learning mill. *Nat. Neurosci.* **17**, 149–150
991 (2014).

992 92. Harris, C. M. & Wolpert, D. M. Signal-dependent noise determines motor planning. *Nature* **394**, 780–784 (1998).

993 93. Osborne, L. C., Lisberger, S. G. & Bialek, W. A sensory source for motor variation. *Nature* **437**, 412–416 (2005).

994 94. Sutton, R. S., McAllester, D. A., Singh, S. P. & Mansour, Y. Policy gradient methods for reinforcement learning with
995 function approximation. In *Adv. Neur. Info. Proc. Sys.*, 1057–1063 (2000).

996 95. Kuo, A. A simple model of bipedal walking predicts the preferred speed–step length relationship. *J. Biomech. Eng.* **123**,
997 264–269 (2001).

998 96. Srinivasan, M. & Ruina, A. Idealized walking and running gaits minimize work. *Proc. Roy. Soc. A* **463**, 2429–2446
999 (2007).

1000 97. Selinger, J. C. & Donelan, J. M. Estimating instantaneous energetic cost during non-steady-state gait. *J. Appl. Physiol.*
1001 **117**, 1406–1415 (2014).

1002 98. Zhou, K. & Doyle, J. C. *Essentials of robust control*, vol. 104 (Prentice hall Upper Saddle River, NJ, 1998).

1003 99. Bertram, J. & Ruina, A. Multiple walking speed-frequency relations are predicted by constrained optimization. *J. theor.
1004 Biol.* **209**, 445–453 (2001).

1005 100. Minetti, A. & Alexander, R. A theory of metabolic costs for bipedal gaits. *J. Theor. Biol.* **186**, 467–476 (1997).

1006 101. Srinivasan, M. Optimal speeds for walking and running, and walking on a moving walkway. *CHAOS* **19**, 026112 (2009).

1007 Acknowledgements

1008 N.S. was funded by the Massachusetts Institute of Technology. M.S. was supported in part by NIH grant R01GM135923-01
1009 and NSF SCH grant 2014506.

1010 **Author contributions statement**

1011 NS initially conceived the central question. NS and MS conceived the theoretical framework, created mathematical models,
1012 performed computations, analyzed the results, and wrote the manuscript. BC contributed additional models and calculations.
1013 All authors reviewed and approved the manuscript.

1014 **Competing interests.**

1015 The authors declare that they have no competing interests.

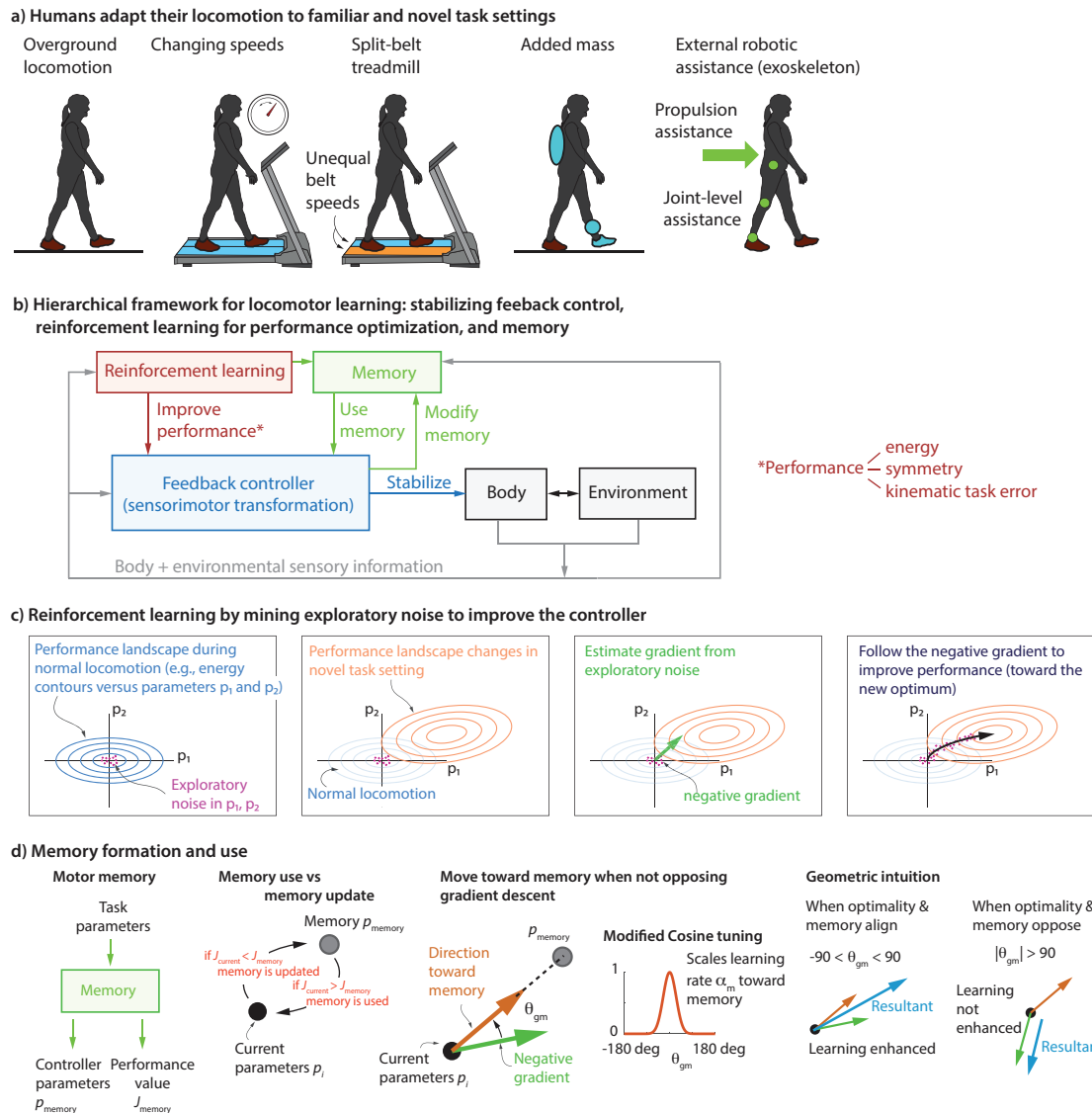
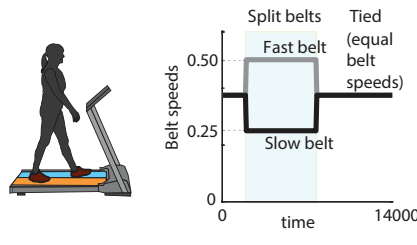


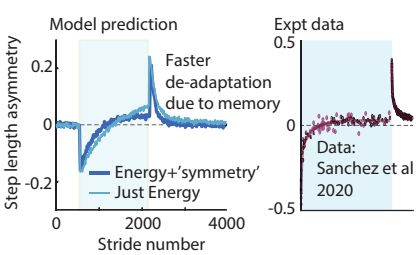
Figure 1. A hierarchical framework for locomotor adaptation. **a.** Humans are able to adapt readily to numerous locomotor task settings, both familiar and novel. **b.** Description of the proposed hierarchical framework, containing three components: (i) the inner loop, represents a fast timescale response due to the stabilizing feedback controller (blue), aimed at avoiding falling; (ii) an outer loop, represents reinforcement learning (red) that tunes the parameters of the inner loop controller to improve some performance objective; (iii) storing and using memories of the learned controllers (green). Alternative adaptation mechanisms may include different performance objectives within the same framework (energy, symmetry, task error) or may replace the feedback controller by a sensorimotor transformation with a state estimator followed by the controller (Fig. 9). **c.** Reinforcement learning by mining exploratory noise to estimate gradient and improve the controller. Initially, the controller parameters p_1 and p_2 are near the optimum of the initial performance landscape (blue). When conditions change, the performance contours change (blue to orange) as does the optimum. Exploratory noise in the controller parameters, allows the learner to estimate the gradient of the performance objective and follow the negative of this gradient to improve performance. **d.** Memory takes in task parameters and returns the stored controller parameters p_{memory} and the associated performance value J_{memory} . We describe how memory is used in concert with gradient-based learning. The control parameters p_i are updated toward memory p_{memory} when doing so improves performance (memory use); memory is updated toward the current parameters otherwise. Updates toward memory is degraded if these updates are not aligned with the gradient, and this degradation is mediated by a modified cosine tuning.

a) Model predictions vs experimental data: Fast and slow transients in split-belt walking predicted by model

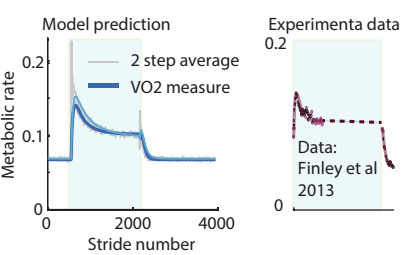
Split-belt speed protocol



Model predicts step length asymmetry

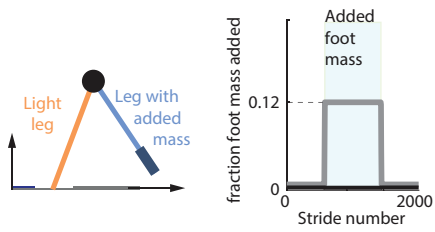


Energy cost changes during adaptation

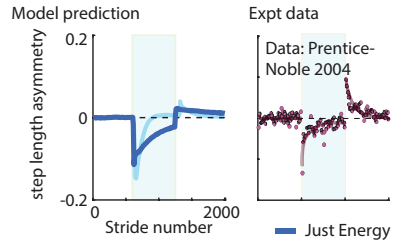


b) Model predictions vs experimental data: Fast and slow transients while walking with an asymmetric foot mass predicted by model

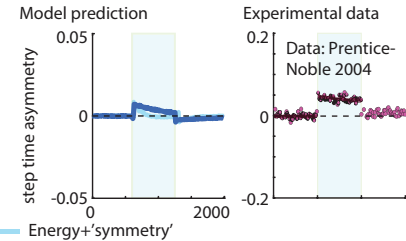
Foot mass adaptation protocol



Step length asymmetry becomes negative

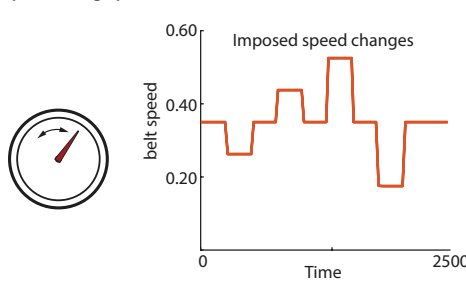


Step time asymmetry becomes positive

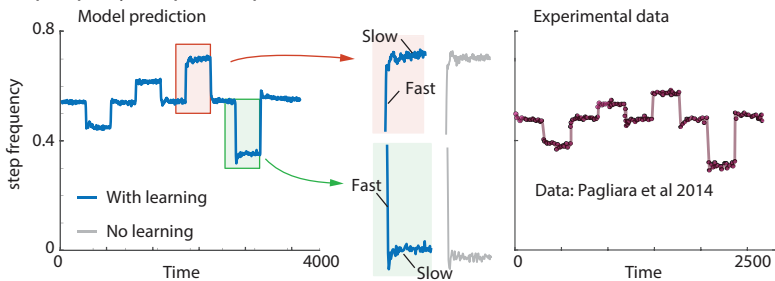


c) Model predictions vs experimental data: Step frequency in response to speed changes predicted by model

Speed change protocol

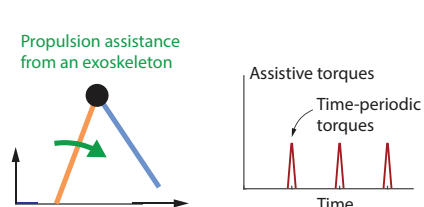


Step frequency in response to speed fluctuations

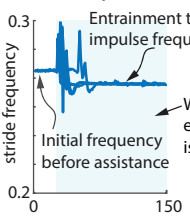


d) Model predictions vs experimental data: Walking with external assistance from an exoskeleton

(d-i) Exoskeleton assistance protocol



(d-ii) Model predicts entrainment



(d-iii) Model can predict phase locking with heelstrike

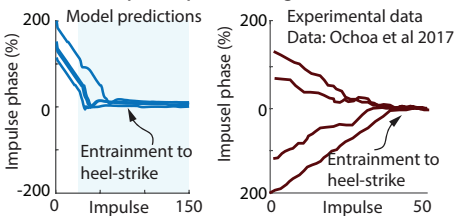
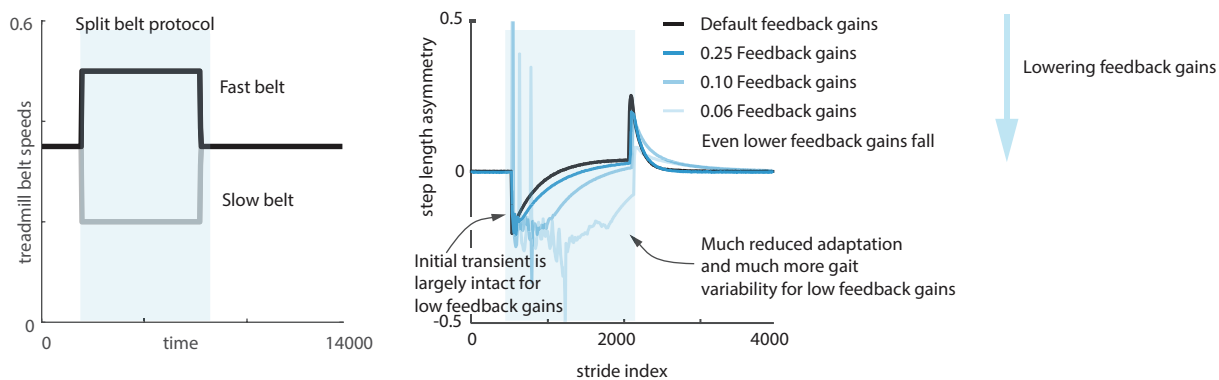


Figure 2. Hierarchical model predicts locomotor adaptation in multiple task settings. **a.** Split-belt walking^{6,45}, that is, with the two belts going at different speeds. Model qualitatively predicts experimental transients in step length asymmetry and metabolic energy during adaptation and de-adaptation. **b.** Walking with an additional mass on one foot⁵. Model qualitatively predicts experimental transients in step length asymmetry during adaptation and de-adaptation. Adaptation phases are shaded in blue in panels a and b. **c.** Walking on a treadmill with abrupt speed changes every 90 seconds²⁸. Model qualitatively predicts experimentally observed step frequency changes. Transients have a fast and slow timescale, with the fast timescale change sometimes undershooting and sometimes overshooting the steady state (red and green detail). Without learning, with just the feedback controller (gray), the fast transient is preserved but the slow transient is replaced by a (noisy) constant. **d-i.** Walking with an exoskeleton that provides periodic propulsive impulses⁴⁸. **d-ii.** Stride period converges to the perturbation period, implying entrainment. Different trajectories starting from different initial conditions are shown. **d-iii.** Perturbation phase converges to zero (heel-strike) in both model predictions and experiment. Different model trajectories show trials starting from different initial conditions. All quantities are non-dimensional. Source data are provided as a Source Data file.

Significance of the stabilizing feedback controller: avoiding falling and improving learning

a) Lower feedback gains results in much lower adaptation and greater gait variability



b) Very low or zero feedback gains can result in falling

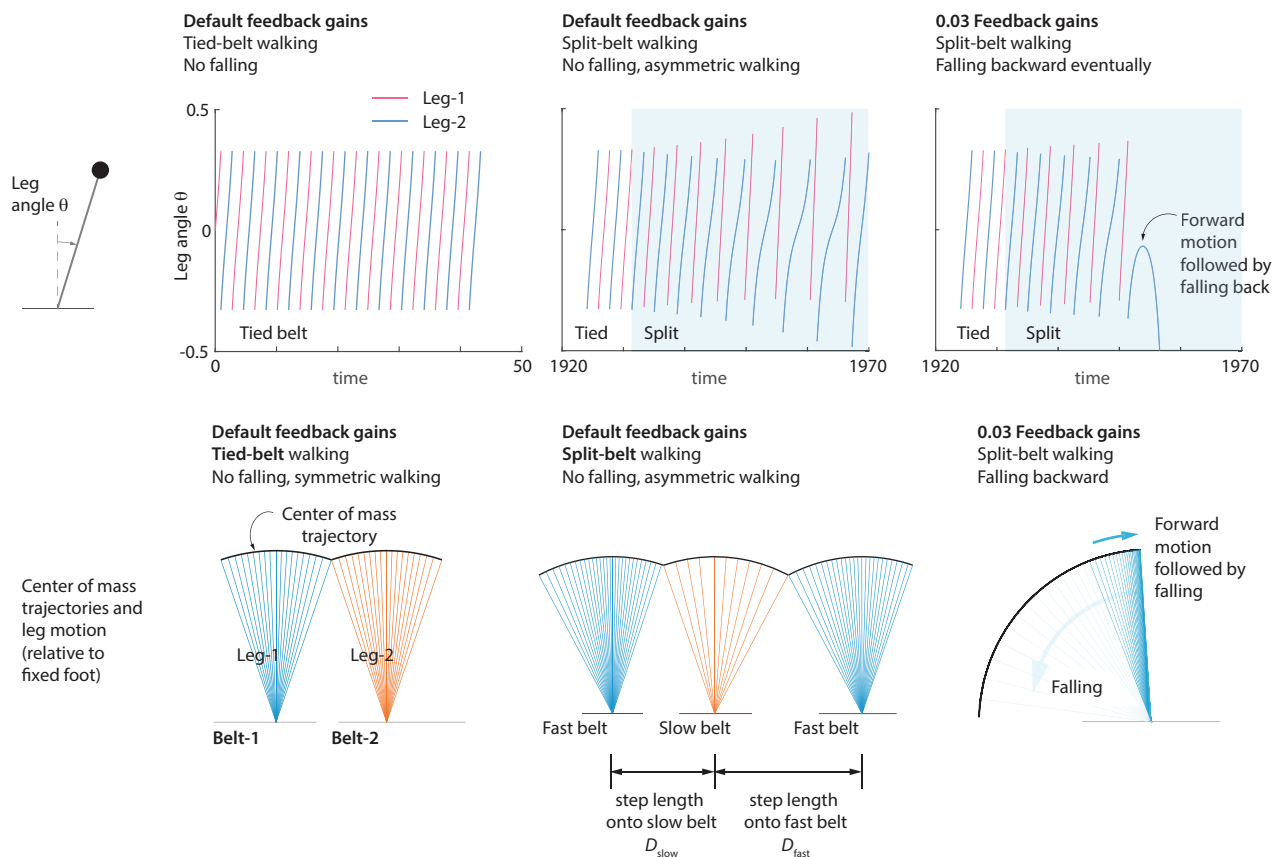


Figure 3. Significance of the stabilizing feedback controller: avoiding falling and improving learning. **a)** The default controller provides robust stability to the biped despite noise and environmental changes. Substantially lowering the feedback gains, all by the same factor, reduces the effective adaptation rate and increases gait variability. The sensory noise in these simulations is fixed across these feedback gain conditions and is applied to velocity feedback to the feedback controller. Adaptation phases are shaded in blue. **b)** Lowering the feedback gains even further results in falling of the biped upon introducing the split-belt perturbation. Three walking patterns are shown: normal tied-belt walking that has symmetric step lengths, split-belt walking with default feedback gains resulting in stable but asymmetric gait, and split-belt walking with much reduced feedback gains resulting in falling. In the bottom-most row, the center of mass trajectories for each stance phase are shown relative to the respective stance belt frame for visualization purposes (so that the split-belt trajectories for the different stance phases are with respect to different frames). Source data are provided as a Source Data file.

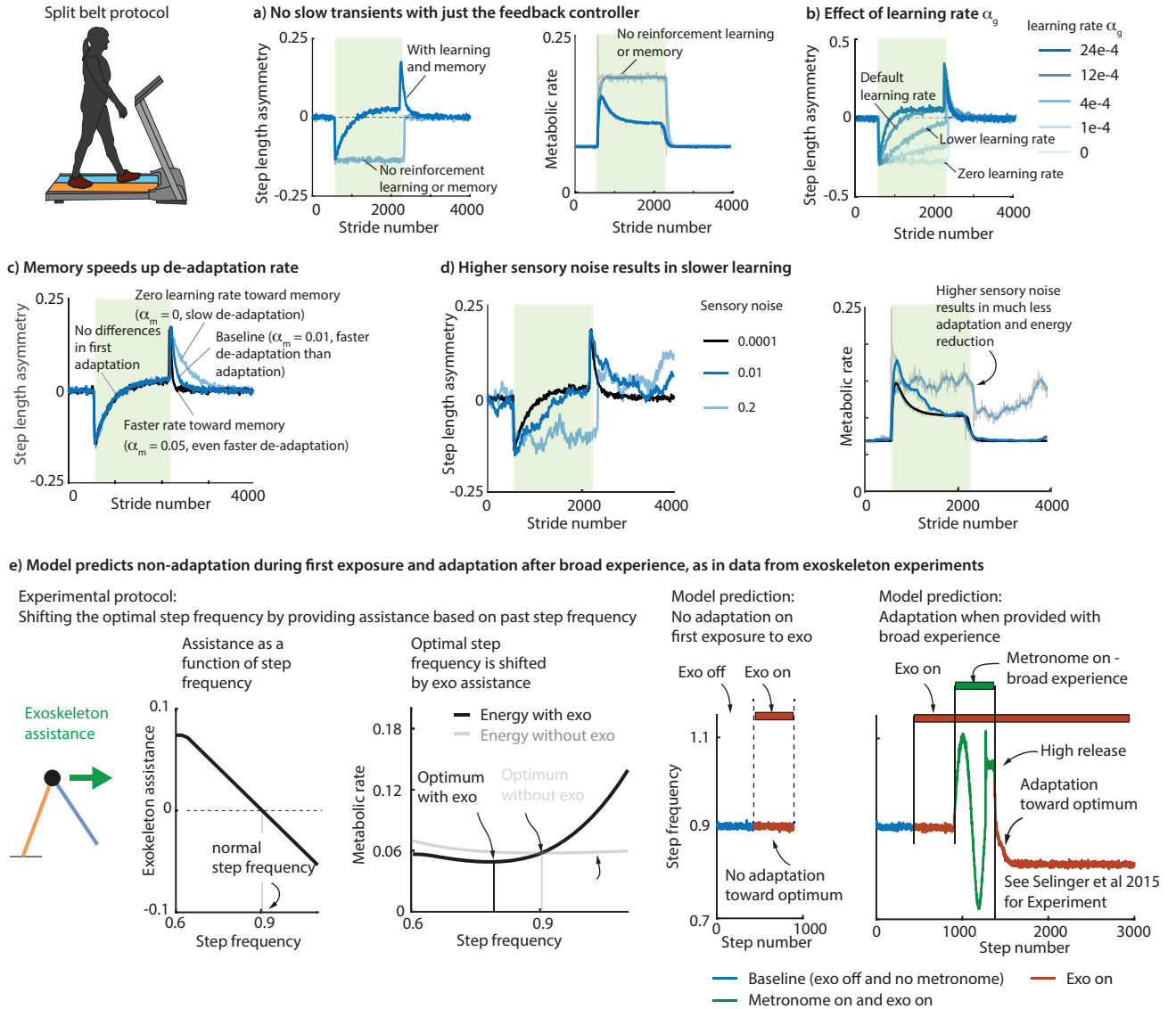


Figure 4. Effect of learning rate, memory and sensory noise: Model captures degraded learning, non-learning, and improving with guided experience. **a.** Stabilizing feedback controller alone only captures the fast learning transient. Addition of reinforcement learner is needed to capture the slow transients. **b.** Increasing the learning rate parameter speeds up learning (for a range of learning rates). **c.** Progress toward memory makes de-adaptation faster than adaptation. **d.** Increasing sensory noise degrades learning for fixed learning rate and fixed exploratory noise, resulting in less learning and less energy reduction. Split-belt adaptation phases are denoted by green shaded region in panels a-d. **e.** Model captures experimental phenomena^{2,8} wherein a human does not adapt to an exoskeleton that provides step-frequency-dependent assistance upon first encounter, but adapts toward the energy optimal frequency when provided with broad experience across a range of frequencies via a metronome-tracking condition. On the right two panels, blue indicates baseline condition without any assistance, red indicates exoskeleton assistance condition, and green indicates metronome-tracking condition in addition to exoskeleton assistance. In the rightmost panels, the 'exo on' condition (red) shows no adaptation before broad experience (green), but shows adaptation after the broad experience. All quantities are non-dimensional. Source data are provided as a Source Data file.

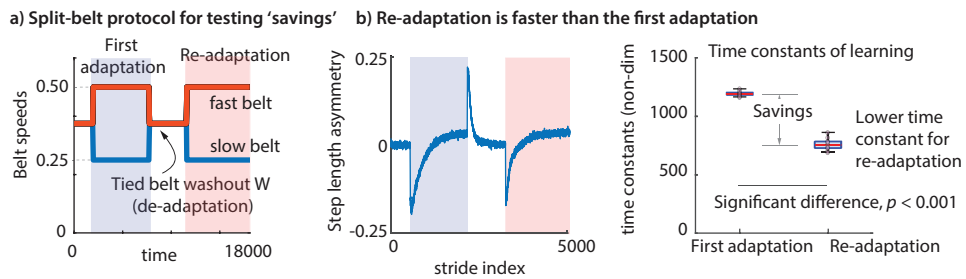
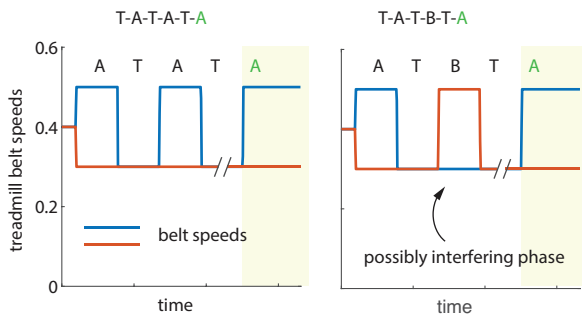


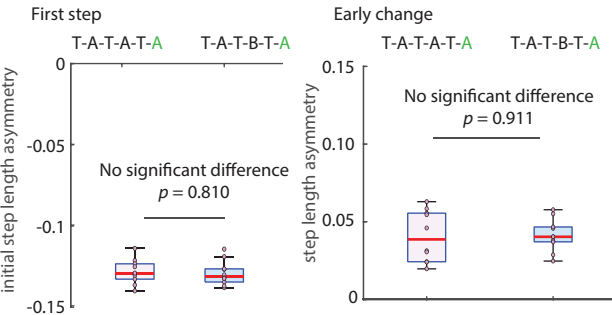
Figure 5. Savings. ‘Savings’ refers to the phenomenon that humans re-adapt faster to a condition (say, split-belt walking) if they have experienced the condition before, even if they have fully de-adapted to normal walking in the intervening time. a) A treadmill protocol with two split-belt adaptation periods with an intervening tied-belt washout de-adaptation phase (W) that brings all the externally observable state variables as well as the current controller back to baseline — but not the internal memory state, which remembers the past learning. First adaptation (blue shaded region) and re-adaptation (red shaded region) transients are shown. b) The model with memory predicts this experimentally observed savings phenomenon⁵¹. Step length asymmetry changes are faster during re-adaptation compared to the first adaptation. The re-adaptation has a smaller initial transient compared to the first adaptation. The time-constants of first adaptation and re-adaptation are computed by fitting a single exponential to the step length asymmetry transients, showing that re-adaptation has a faster time-constant. Source data are provided as a Source Data file. See Supplementary Table 1 for statistical details of comparisons. All box-plots show the median (red bar), 25-75% percentile (box), range (whiskers), and individual data points (pink circles).

Two experiments for testing 'interference'

a) Model predicts no significant interference when comparing the final 'A' in the protocols T-A-T-A-T-A-T-A and T-A-T-B-T-A
(as in Malone and Bastian, 2011)

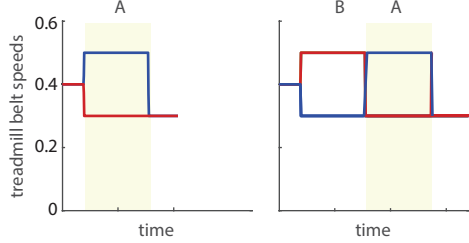


Model predictions: No significant difference in first step or early change with or without the counter perturbation

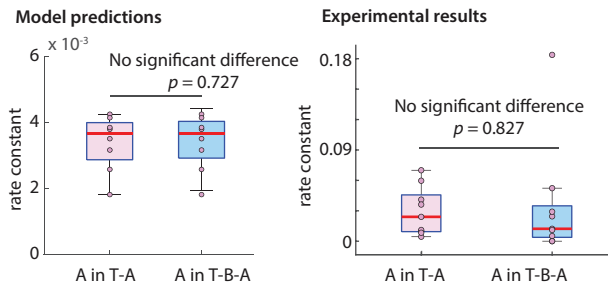


b) Model predicts behavior in new experiments comparing adaptation A and B-A

Comparing two adaptation protocols



No significant difference in adaptation rate constant with and without prior experience with counter perturbation



Initial response is significantly higher immediately after prior experience with a counter perturbation (without washout)

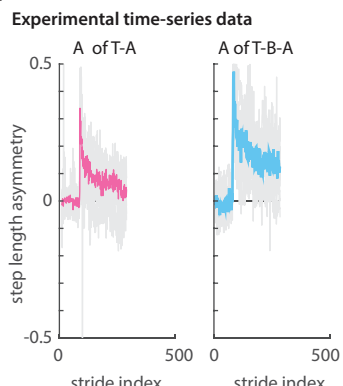
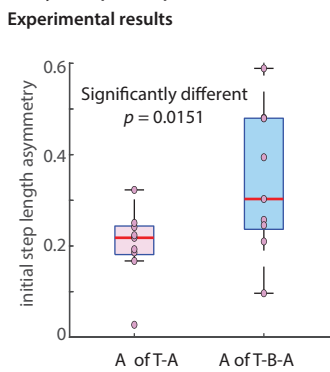
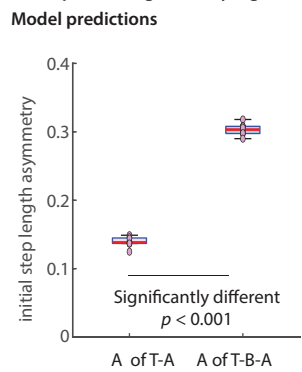
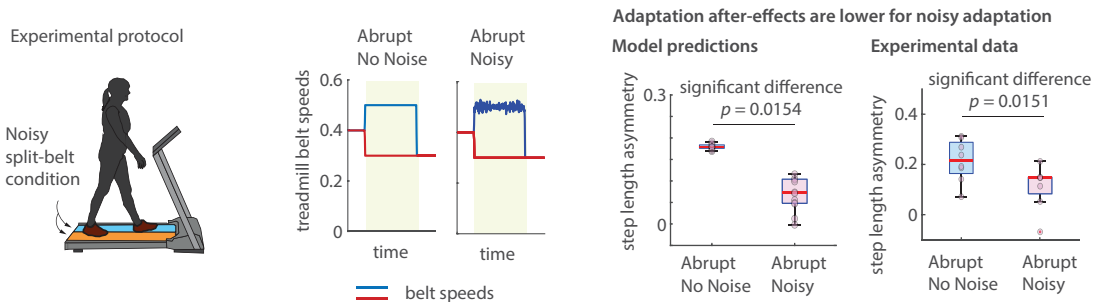


Figure 6. Interference. 'Anterograde interference' refers to the phenomenon where humans sometimes adapt slower to a condition A when they were previously exposed to the opposite condition B, that is, with the belt speed differences reversed between the two belts. a) We performed simulations of two split-belt adaptation protocols: first, T-A-T-A-T-A, alternating between tied-belt conditions T and the split-belt condition A, and second, T-A-T-B-T-A, where one of the A phases is replaced with the opposite condition B. We compare the adaptation between the two protocols during the final A phase (denoted as yellow shaded region). We find that the two protocols are not significantly different in their initial response to the perturbation or the early change in the step length asymmetry for the final adaptation period (yellow shaded region), as shown by Malone et al⁵¹. b) To test if this non-interference remains in the absence of washout, we performed prospective experiments in the absence of such a tied-belt washout phase: we compared protocols T-A with T-B-A with both simulations and human participant experiments. In experiments, we found that the initial step length asymmetry (first step of A) was significantly higher when B was present and the time constant of adaptation during A was not significantly different under the two conditions. This confirmed our model simulations, which predicted that the initial transients for A will be higher after B. The model also predicted no statistically significant difference in the adaptation rate constant in the presence of inter-participant variability of magnitude similar to that in the experiment. Box-plot shows median, 25-75% percentile and range. Source data are provided as a Source Data file. All box-plots show the median (red bar), 25-75% percentile (box) range (whiskers), and individual data points (pink circles). The time-series shows median as thick colored line and light gray lines are individual participant data overlaid. See Supplementary Table 1 for statistical details of comparisons.

Effect of environmental noise on learning

Model predicts non-monotonic effect of belt noise on split belt walking, confirmed by experiment

a) Noise can degrade adaptation after-effects (comparison with new data from the present study)



b) Noise can improve adaptation after-effects (Comparison with data from Torres-Oviedo and Bastian, 2012)

'Gradual Noisy' and 'Abrupt No Noise' protocols produce larger after-effects than 'Gradual No Noise' protocol

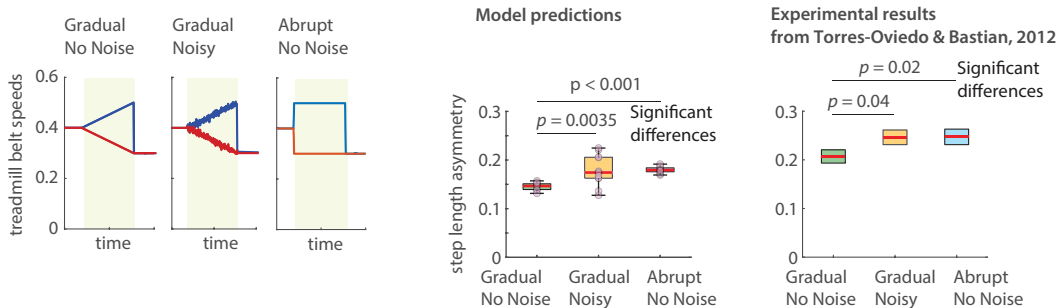
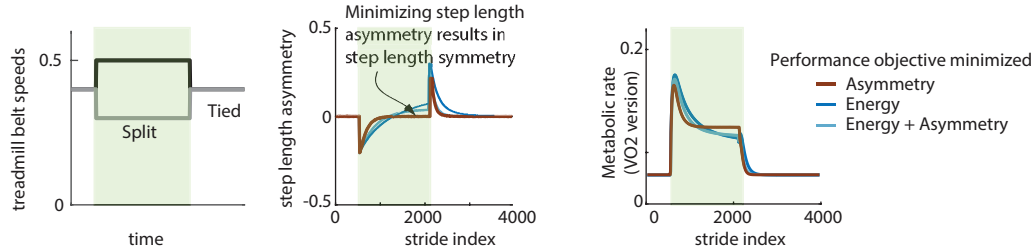


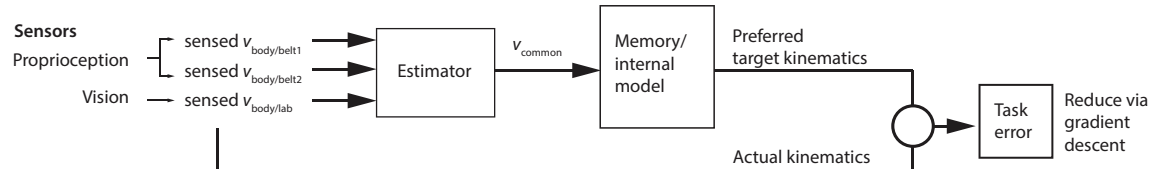
Figure 7. Split-belt learning can be degraded or enhanced depending on noise structure. a) Split-belt adaptation with and without belt-noise are compared. Adaptation phases are shaded in light green. The speed fluctuations in the noisy split-belt condition are continuous and piecewise linear and happen roughly every step. Model predicts that when the belt noise is high enough, adaptation can be degraded, as judged by lower post-adaptation after-effects. The post-adaptation after-effects shown are the initial step length asymmetry when the tied-belt condition starts after the split-belt adaptation. We performed model-guided prospective human experiments that confirmed these predictions: p value showing significant difference is from one-tailed t-test (unpaired, $t(df) = -2.41(14)$, $p = 0.0151$). b) Torres-Oviedo and Bastian²⁰ found that appropriately structured noise accompanied by gradual speed change can enhance adaptation, as measured by post-adaptation after-effects: box plot with these prior experimental results²⁰ shows mean (red line) and standard error (box). Our model captures this behavior. All box-plots show the median (red bar), 25-75% percentile (box) range (whiskers), and individual data points (pink circles). See Supplementary Table 1 for full statistical details of comparisons. Source data are provided as a Source Data file.

Alternatives to minimizing energy: Minimizing step length asymmetry or kinematic task error

a) Minimizing step length asymmetry alone versus minimizing energy



b) Defining kinematic task error as deviation from equivalent tied belt walking kinematics



c) Model predictions for minimizing kinematic task error

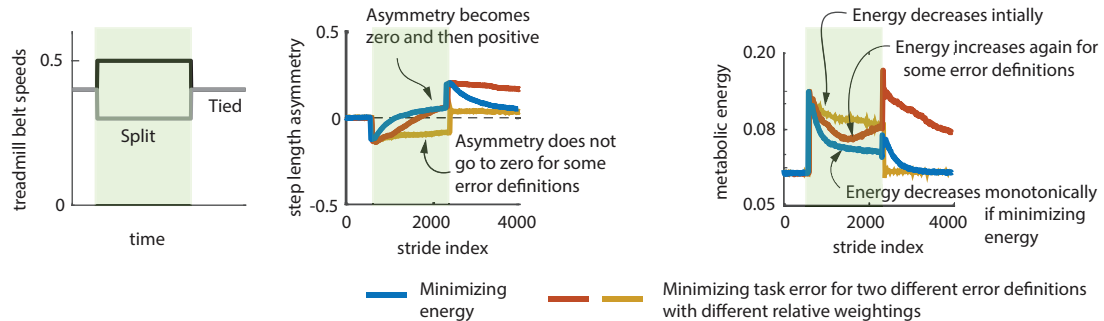
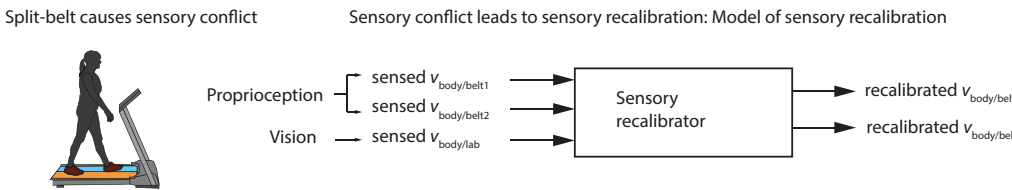


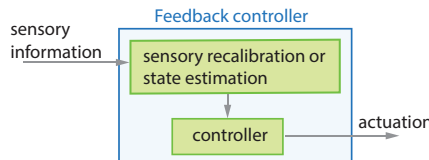
Figure 8. Alternatives to energy minimization: minimizing asymmetry or kinematic task error. **a)** As an alternative to an energy objective, minimizing step length asymmetry as the only objective during split-belt adaptation results in a perfectly symmetric gait in the model, which conflicts with the positive step length asymmetry found in experiment as well as when predicted by an energy minimization⁴⁵. **b)** As another alternative to an energy objective, we formalize the minimization of kinematic task error as minimizing deviation from preferred walking kinematics defined for each speed. A single common belt speed is estimated by a state estimator using sensed body speeds relative to the lab and the belt (vision and proprioception). The task error is deviation from kinematics at that estimated speed under tied-belt conditions, drawn from memory. **c)** Model predictions for minimizing just task error without an energy objective; two different weightings are used for different components of the kinematic error (red and yellow). Energy minimization is shown for comparison (blue). For the task error predictions, one of either step length asymmetry or energy trends disagree with split belt adaptation experiments⁴⁵: either the step length asymmetry stops well short of symmetry while decreasing energy somewhat (yellow), or the energy transients are not monotonically decreasing (red). Source data are provided as a Source Data file. Light green shaded region in all panels is the period of split-belt adaption.

Alternative to minimizing energy: Sensory recalibration for proprioceptive realignment

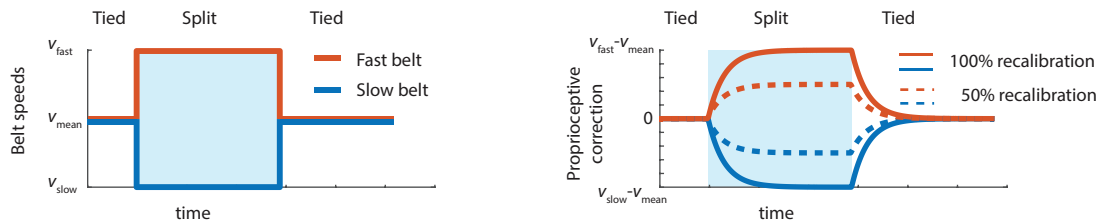
a) Sensory recalibration



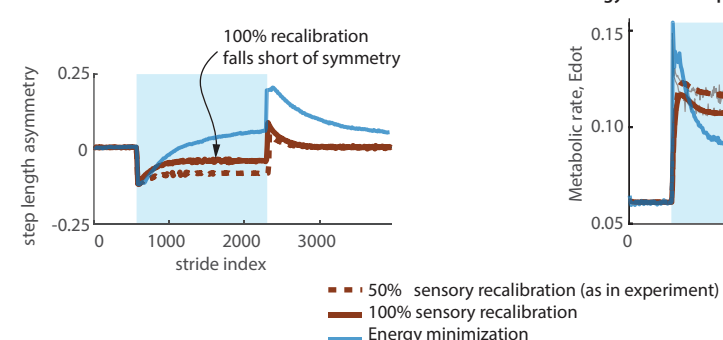
b) Replacing the feedback controller by a sensorimotor transformation that includes sensory recalibration



c) Proprioceptive realignment due to sensory recalibration



d) Model predictions: Proprioceptive realignment reduces step length asymmetry but falls short of symmetry



e) Model predictions: Proprioceptive realignment coincidentally reduces energy even when energy is not the optimized objective

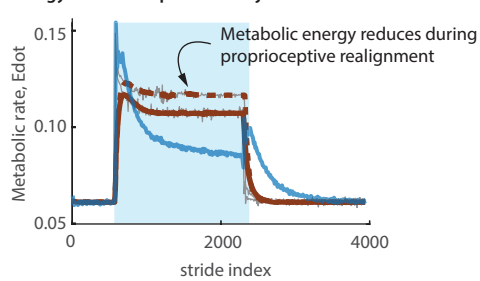
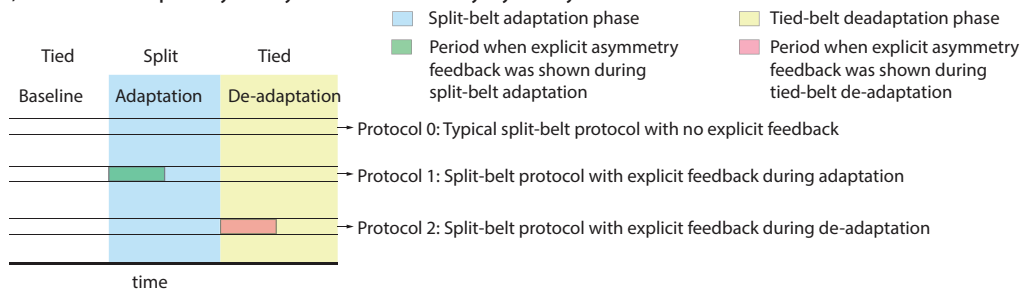


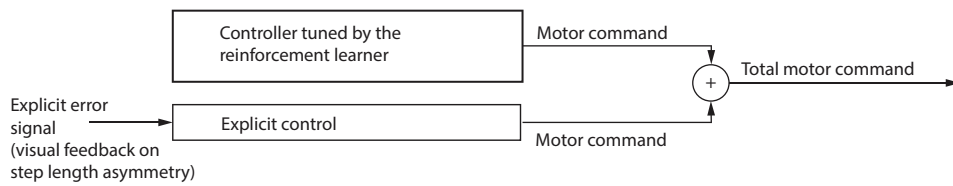
Figure 9. Alternative to energy minimization: Sensory recalibration via proprioceptive realignment. **a)** As an alternative to energy minimization, we considered sensory recalibration via proprioceptive realignment as a hypothesis for adaptation. This recalibration realigns the proprioception from the two legs to conform with the expectation that both legs usually are on the same surface with a common speed, rather than surfaces with different speeds. The proprioceptive recalibrator takes in the sensory information from proprioceptors of the two legs and vision and computes a recalibrated version of the proprioceptive information. **b)** The recalibrated sensory information is used by the the stabilizing controller, so the direct feedback controller of Fig. 1 is replaced by a more general sensorimotor transformation. **c)** Proprioceptive correction for each leg shown as a function of time for a particular split-belt protocol. This correction is subtracted from the initial proprioceptive estimate to obtain the recalibrated proprioception. The correction for the fast leg is positive and that for the slow leg is negative. 100% recalibration corresponds to completed proprioceptive realignment and 50% recalibration is close to that observed in experiment⁴². **d)** Using the recalibrated proprioception as feedback in the stabilizing controller results in the reduction of step length asymmetry, but even 100% recalibration does not result in symmetry or positive step length asymmetry. Thus, the model predicts that proprioceptive realignment cannot be fully responsible for split-belt adaptation. **e)** Proprioceptive realignment also reduces energy coincidentally even without energy being an explicit objective in this situation. Source data are provided as a Source Data file. Light blue shaded region in panels c-e is the period of split-belt adaption.

Modeling interaction of implicit and explicit adaptation during locomotion

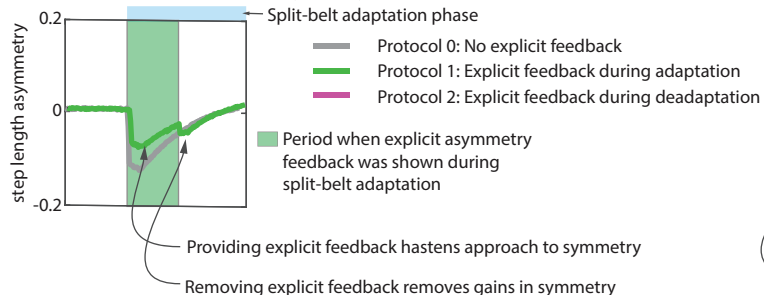
a) Protocols with explicit asymmetry feedback for voluntary asymmetry reduction



b) Putative mechanism to accommodate explicit asymmetry feedback



c) Adaptation with explicit asymmetry reduction (protocol 1)



d) De-adaptation with explicit asymmetry reduction (protocol 2)

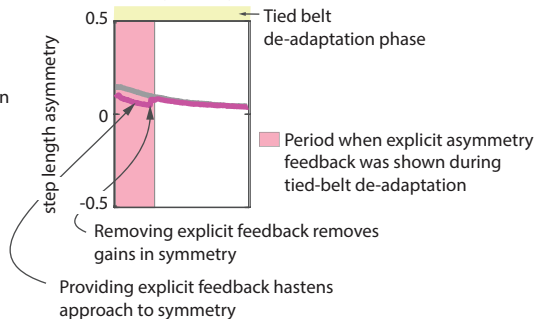


Figure 10. Interaction with explicit feedback. **a)** Three different split-belt protocols are compared. Protocol 0 which is a typical split-belt protocol with no explicit feedback about step length asymmetry. In protocols 1 and 2, participants are shown visual feedback of step length asymmetry on a screen and asked to reduce it explicitly, either partly through the adaptation phase (protocol 1) or partly through the de-adaptation phase (protocol 2). **b)** Explicit control is modeled as a module that adds to the nominal step length of the ‘implicit controller’ and this correction is proportional to the step length asymmetry on the previous step. The explicit and implicit modules are in parallel, and the implicit learner only knows about the motor command from the implicit feedback controller that it tunes. Having the explicit feedback improves progress to symmetry during **c)** adaptation and **d)** de-adaptation but this symmetry improvement is lost when the explicit feedback is removed, as found in experiment¹⁰. Source data are provided as a Source Data file.

Additional information

¹⁰¹⁶ **Supplementary Methods** is available for this paper.

¹⁰¹⁷ **Correspondence and request for materials** should be addressed to NS or MS.

¹⁰¹⁸

¹⁰¹⁹